Open Archive TOULOUSE Archive Ouverte (OATAO)
OATAO is an open access repository that collects the work of Toulouse researchers and makes it freely available over the web where possible.

This is an author-deposited version published in : http://oatao.univ-toulouse.fr/
Eprints ID : 3159

To link to this article : DOI :10.1105/tpc.108.060830
URL : **http://dx.doi.org/10.1105/tpc.108.060830**

To cite this version :
Wang, Hua and Schauer, Nicolas and Usadel, Bjoern and Frasse, Pierre and Zouine, Mohamed and Hernould, Michel and Latché, Alain and Pech, Jean-Claude and Fernie, Alisdair R. and Bouzayen, Mondher (2009) *Regulatory Features Underlying Pollination-Dependent and -Independent Tomato Fruit Set Revealed by Transcript and Primary Metabolite Profiling.* The Plant Cell, vol.21 . pp. 1428-1452. ISSN 1040-4651

Any correspondance concerning this service should be sent to the repository administrator: staff-oatao@inp-toulouse.fr.

Regulatory Features Underlying Pollination-Dependent and -Independent Tomato Fruit Set Revealed by Transcript and Primary Metabolite Profiling

Hua Wang,[a,b] Nicolas Schauer,[c] Bjoern Usadel,[c] Pierre Frasse,[a,b] Mohamed Zouine,[a,b] Michel Hernould,[d] Alain Latché,[a,b] Jean-Claude Pech,[a,b] Alisdair R. Fernie,[c] and Mondher Bouzayen[a,b,1]

[a] Université de Toulouse, Institut National Polytechnique - Ecole Nationale Superieure Agronomique Toulouse, Génomique et Biotechnologie des Fruits, Castanet-Tolosan F-31326, France

[b] Institut National de la Recherche Agronomique, Génomique et Biotechnologie des Fruits, Chemin de Borde Rouge, Castanet-Tolosan, F-31326, France

[c] Max-Planck-Institut für Molekulare Pflanzenphysiologie, 14476 Potsdam-Golm, Germany

[d] Unité Mixte de Recherche 619 Biologie du Fruit, Institut National de la Recherche Agronomique, Université de Bordeaux, Institut de Biologie Végétale Moléculaire, 33883 Villenave d'Ornon, France

Indole Acetic Acid 9 (IAA9) is a negative auxin response regulator belonging to the *Aux/IAA* transcription factor gene family whose downregulation triggers fruit set before pollination, thus giving rise to parthenocarpy. In situ hybridization experiments revealed that a tissue-specific gradient of *IAA9* expression is established during flower development, the release of which upon pollination triggers the initiation of fruit development. Comparative transcriptome and targeted metabolome analysis uncovered important features of the molecular events underlying pollination-induced and pollination-independent fruit set. Comprehensive transcriptomic profiling identified a high number of genes common to both types of fruit set, among which only a small subset are dependent on IAA9 regulation. The fine-tuning of *Aux/IAA* and *ARF* genes and the downregulation of *TAG1* and *TAGL6* MADS box genes are instrumental in triggering the fruit set program. Auxin and ethylene emerged as the most active signaling hormones involved in the flower-to-fruit transition. However, while these hormones affected only a small number of transcriptional events, dramatic shifts were observed at the metabolic and developmental levels. The activation of photosynthesis and sucrose metabolism-related genes is an integral regulatory component of fruit set process. The combined results allow a far greater comprehension of the regulatory and metabolic events controlling early fruit development both in the presence and absence of pollination/fertilization.

INTRODUCTION

Fruit development is a genetically programmed process, unique to flowering plants, which provides a suitable environment for seed maturation and seed dispersal. Given the fundamental nature of both the dietary and biological significance of fruit, it is unsurprising that the molecular dissection of fruit development has recently received considerable interest (Giovannoni, 2001; Pandolfini et al., 2007; Serrani et al., 2008). The fruit is the result of the development of the ovary, and fruit organogenesis originates from a flower primordial. The mature flower can either be fertilized and develop into a fruit or, in the absence of successful pollination, can enter the abscission process. The onset of the development of an ovary into fruit, the so-called fruit set, thus constitutes an essential mechanism for fruit production. Despite the importance of the fruit set process, most research effort to date has been dedicated to the processes of fruit maturation (Alba et al., 2005) and fruit growth (Carrari et al., 2006), while the molecular mechanisms underlying the onset of ovary development itself remain relatively poorly defined.

In normal fruit development, the initiation of fruit set depends on the successful completion of pollination and fertilization; this suggests that both pollination and seed-derived signals are required for fruit initiation and subsequent development. Fruit growth and shape are known to be modified by differences in seed genotype and seed number (Sedgley and Griffin, 1989). However, the signals that trigger fruit growth after fertilization remain unknown. Unfavorable conditions, such as extreme temperatures, may prevent pollination and hence also fruit set. Mild temperature stress, leading to loss of pollen viability, can result in the production of underfertilized puffy fruits of poor quality, while severe temperature stress can completely abolish fruit set. In tomato (*Solanum lycopersicum*) and many other species, a major limiting factor for fruit set is the extreme sensitivity of microsporogenesis and pollination to moderate fluctuations in temperature and humidity (Picken, 1984). Hence, parthenocarpy, the growth of the ovary into a seedless fruit in the absence of pollination and fertilization, has long been recognized as an important trait that circumvents the problems of low fruit set in

[1] Address correspondence to bouzayen@ensat.fr.

harsh environmental conditions (Gorguet et al., 2005). Fertilization-independent fruit set can occur either naturally (genetic parthenocarpy) or by induction via exogenous application of phytohormones, such as auxin and gibberellins (GAs), to the flower (Gustafson, 1936; Coombe, 1960). The presence of both germinated pollen and developing seeds appears to be essential for fruit growth and development, since they probably serve as sources of phytohormones that are, most likely, continuously required throughout seed and fruit formation (Nitsch, 1970; Talon et al., 1992; Ozga et al., 2002). In keeping with this hypothesis, elevated endogenous phytohormone levels have been observed during parthenocarpic fruit set (George et al., 1984; Talon et al., 1992). Accordingly, parthenocarpy can be induced in diverse agricultural species not only by the exogenous application of auxins, cytokinins, or GAs (Gillaspy et al., 1993; Vivian-Smith and Koltunow, 1999; Serrani et al., 2007) but also by increasing either auxin levels or auxin response in ovaries and ovules (Carmi et al., 2003; Rotino et al., 2005) or by increasing the GA response (Potts et al., 1985). Recent molecular analyses of fertilization-independent fruit formation in both tomato and *Arabidopsis thaliana* have, however, identified auxin signaling as one of the early events in the fruit initiation cascade. Furthermore, components of the auxin signaling pathway are also involved in repressing fruit initiation until the fertilization cue (Vivian-Smith et al., 2001; Wang et al., 2005; Goetz et al., 2006). When considered together, these data demonstrate that hormones, such as auxin, play an important role in fruit initiation. However, the exact mechanism by which auxin promotes fruit initiation and the nature of the genes that control fruit set remain an open question.

We previously reported that downregulation of *IAA9*, a member of the *Aux/IAA* transcription factor gene family encoding a negative auxin response regulator, in tomato resulted in pollination-independent fruit set giving rise to parthenocarpy (Wang et al., 2005). In this study, taking advantage of this unique biological tool, we sought to uncover the molecular events underlying the process of fruit set via a combined transcriptomic and metabolomic approach. Our study reveals that IAA9 closely regulates the initiation of fruit set by establishing a spatial expression gradient whose release triggers the flower-to-fruit transition. The comparative analysis at the transcriptomic and metabolic levels of pollination-induced natural fruit set and fertilization-independent fruit set identifies auxin and ethylene signaling, as well as photosynthesis and sugar metabolism, as major events of the fruit set program and potential components of the regulatory mechanism underlying this developmental process. These data are discussed in comparison to current models of fruit set as well as within the context of the development of future strategies for the biotechnological exploitation of parthenocarpy.

RESULTS

Fertilization-Independent Fruit Set in *AS-IAA9*

MicroTom tomato lines downregulated in the expression of the *IAA9* gene (*AS-IAA9*) exhibit precocious fruit set prior to anthesis, resulting in parallel fruit and flower development (Figure 1A) and uncoupling fruit set from pollination, leading to parthenocarpy

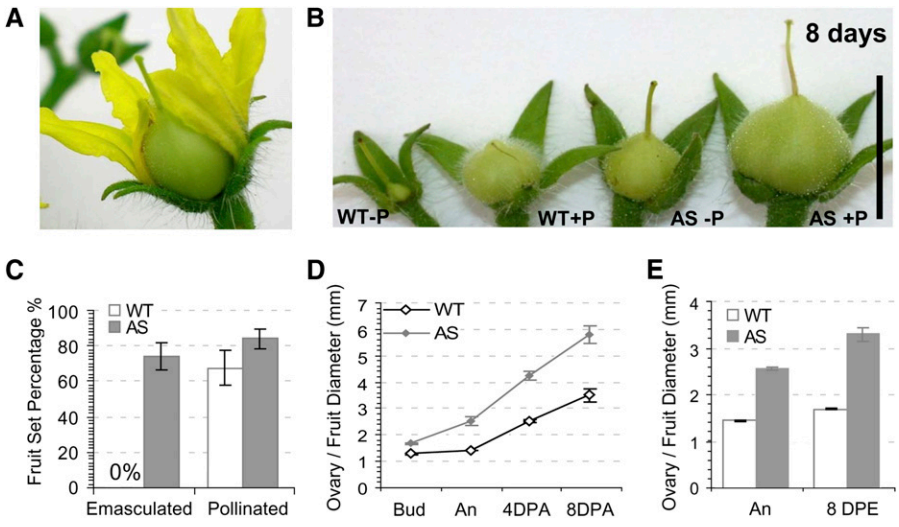

Figure 1. Comparison of Wild-Type and *AS-IAA9* Ovary/Fruit Development during Fruit Set.

(A) *AS-IAA9* lines exhibit precocious fruit set prior to anthesis, resulting in abnormal parallel development of fruit and flower at anthesis stage.
(B) Impact of pollination on fruit size at 8 DPA. +P, pollinated; −P, nonpollinated. Bar = 8 mm.
(C) Percentage of fruit set (the transition from flower to fruit and subsequent fruit development) from emasculated and pollinated flowers in wild-type and *AS-IAA9* lines.
(D) Ovary/fruit diameter in wild-type and *AS-IAA9* lines at anthesis (An) and 8 d postemasculation (DPE).
(E) Accelerated ovary-fruit enlargement in *AS-IAA9* (AS) compared with the wild type.
In **(C)** to **(E)**, error bars represent ± SE of three independent trials, for each trial $n \geq 20$. AS, *IAA9*-antisense lines; Bud, flower bud; An, anthesis.

(Wang et al., 2005). The rate of successful fruit set of emasculated *AS-IAA9* lines (75%) was similar to that observed in the wild type (68%) under natural pollination conditions (Figure 1C). At 8 d postanthesis (DPA), unpollinated *AS-IAA9* young fruits and naturally pollinated wild type had similar size (Figure 1B). Manual pollination stimulated the development of *AS-IAA9* fruit, leading to a fruit size at 8 DPA that were on average 76% bigger than *AS-IAA9* emasculated fruit or wild-type naturally pollinated ones (Figures 1D and 1E). Moreover, Figure 1D indicates that from bud stage onward, *AS-IAA9* displayed accelerated ovary fruit enlargement compared with the wild type. Taken together, these data indicated that pollination of *AS-IAA9* has no significant impact on the rate of fruit set, whereas it substantially promotes fruit enlargement.

Downregulation of *IAA9* Affects Flower/Ovary Development

Given that fruit organogenesis is initiated from the floral primordia, light microscopy analysis was performed to investigate early fruit organogenesis in the wild type and *AS-IAA9*. Figures 2A and 2B reveal that the floral meristem is larger in *AS-IAA9* compared with the wild type, and comparison of 2-mm-long flower buds (Figures 2C and 2D) revealed that the wild type exhibits fused carpels while, at the same size, carpels are still growing toward fusion in *AS-IAA9*. When flower buds are 4 mm long, the nucellus in the wild type is completely embedded in the integument, while, in *AS-IAA9*, the integument is still in the process of surrounding the nucellus (Figures 2E and 2F). These observations indicate that the *AS-IAA9* flower organ corresponds to a more juvenile stage than the wild type and that organ differentiation is not more advanced in the *IAA9*-downregulated lines but rather that the organ exhibits larger growth. Mature *AS-IAA9* flowers (anthesis stage) contained a higher proportion of aborted pollen grains (Figure 2H) than the wild type (Figure 2G), while those not aborted were significantly larger and more intensely colored than in the wild type. However, the latter observation is largely in keeping with our previous observation that *AS-IAA9* pollen retains the capacity to fertilize emasculated wild-type flowers (Wang et al., 2005).

Spatial and Temporal Regulation of *IAA9* Expression during Natural Fruit Set

In situ hybridization during wild-type flower/ovary development and fruit set revealed that *IAA9* mRNA distribution was detectable in the whole floral meristem but was more abundant in emerging organs, such as stamen and carpel (Figure 3B). In the emerging petals, the signal intensity was higher on the adaxial sides. A control hybridization using the sense probe showed no signal (Figure 3A). Though unevenly distributed, the *IAA9* mRNA signal was detected across all flower tissues but exhibited a steady increase throughout flower development peaking at anthesis (Figures 3C to 3G). At these stages, accumulation of the *IAA9* transcript formed a gradient wherein the signal is strongest in ovule, sporogenous tissue, tapetum, petals, vascular bundles, developing style, placenta, and funiculus, but, by contrast, the signal was weak in sepals, ovary wall, and the columella. Successful pollination and fertilization triggered the dissipation of the *IAA9* transcript gradient, which tended to spread across the developing fruit leading to a net decrease in transcript abundance in the placenta, funiculus, and inner integument of embryonic sac (Figures 3H to 3K). Conversely, in the absence of pollination, emasculated flowers retained the original transcript gradient associated with arrest of fruit development (Figures 3L to 3O). A close examination of the ovule confirmed

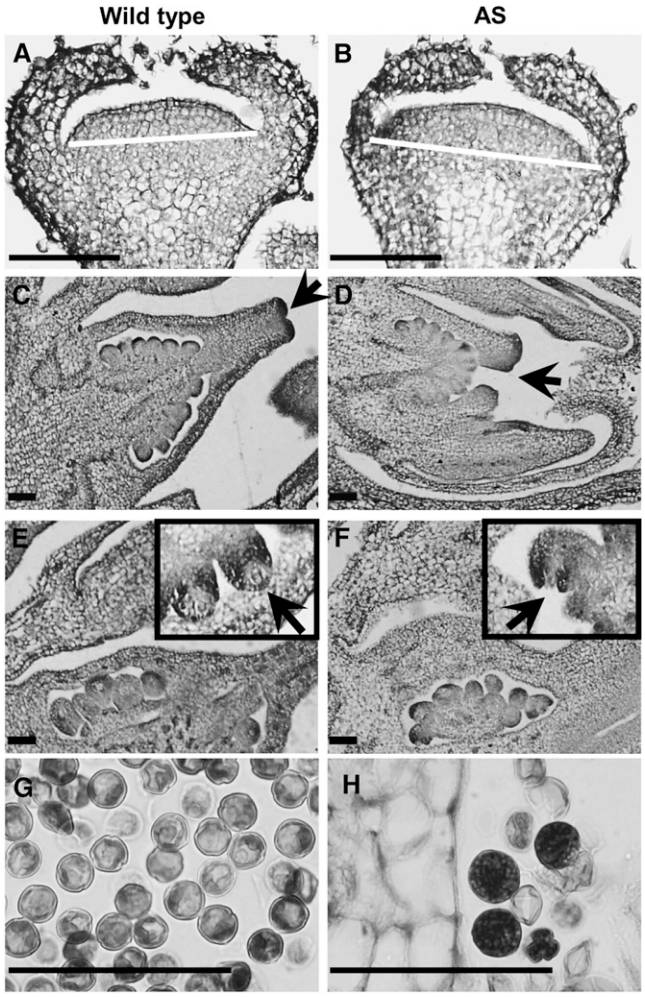

Figure 2. Histological Analysis of Organ Differentiation Program in Wild-Type and *AS-IAA9* Flowers.

(A) and **(B)** Floral meristem is larger in *AS-IAA9* line (AS) than in the wild type as indicated by white bars.

(C) and **(D)** In 2-mm-long flower buds, wild-type lines exhibit fully fused carpels, whereas at the same size, carpels are still growing toward fusion (arrows) in *AS-IAA9*.

(E) and **(F)** In 4-mm-long flower buds, the nucellus is already completely enveloped by the integuments in the wild type, whereas it is still not fully covered by the integuments in *AS-IAA9* lines (insets).

(G) and **(H)** In mature flowers (anthesis stage), a high proportion of pollen grains are aborted in antisense lines compared with the wild type. Nonaborted pollens are significantly bigger and intensely colored in antisense lines compared with the wild type. Bars = 100 μm.

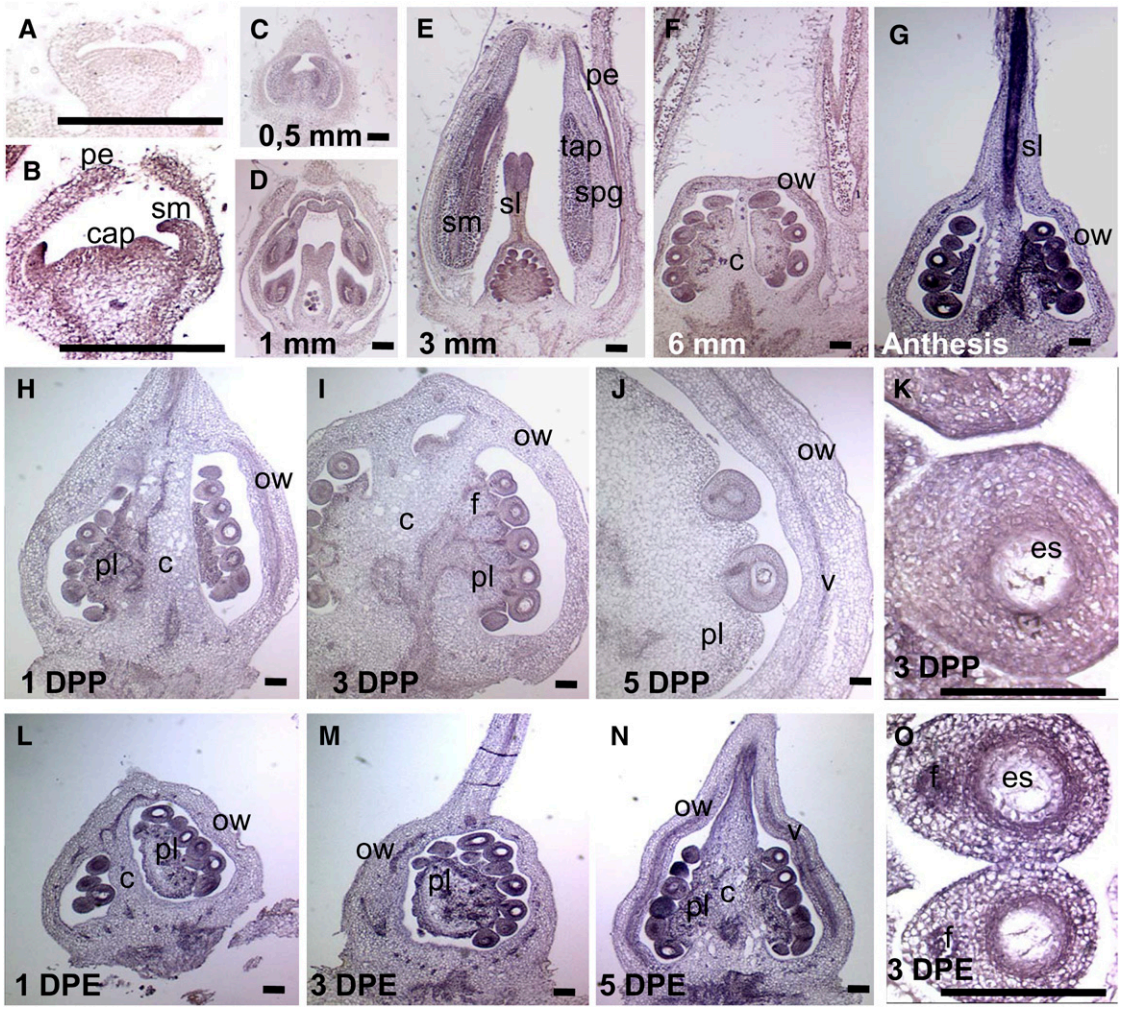

Figure 3. In Situ Hybridization Reveals That Pollination Triggers the Release of the *IAA9* Transcript Gradient.

(A) Low background signal detected in control hybridization experiment performed with *IAA9* sense probe.
(B) *IAA9* mRNAs are distributed all over the floral meristem, with higher accumulation in emerging organs, such as petals, stamen, and carpel. Signal intensity is higher in the adaxial sides of the emerging stamen.
(C) to **(G)** *IAA9* mRNA signal increases throughout flower development with uneven distribution leading to the formation of a gradient peaking at anthesis stage. Flowers from all the stages analyzed were put in the same slide and were therefore developed for the same amount of time.
(H) to **(J)** Pollinated ovaries at 1, 3, and 5 d after pollination (DPP). Pollination results in a rapid release of the *IAA9* gradient leading to a net decrease in *IAA9* mRNA accumulation in the placenta, funiculus, and inner integument of embryonic sac.
(K) Close-up examination of fertilized ovule. Successful fertilization releases the *IAA9* mRNA gradient, resulting in a spreading of the *IAA9* signal all over the developing ovule.
(L) to **(N)** Emasculated ovaries at 1, 3, and 5 DPE. In the absence of pollination, emasculated flowers retain the *IAA9* expression gradient and display an arrest of ovary development.
(O) Close-up examination of unfertilized ovule shows that 3 d after emasculation, a strong *IAA9* mRNA gradient is maintained with a high signal detected in cell layers of inner integuments and funiculus tissues.
Magnification is ×5 in **(C)** to **(J)** and **(L)** to **(N)** and ×40 in **(A)**, **(B)**, **(K)**, and **(O)**. Bars = 100 μm. sp, sepal; sm, stamen; cap, carpels; sl, style; spg, sporogenous tissue; tap, tapetum; c, columella; ow, ovary wall; pl, placenta; f, funiculus; v, vascular bundles; es, embryo sac.

that after flower emasculation, unfertilized ovules displayed a strong gradient in *IAA9* transcript abundance, which maintains a high level of *IAA9* transcripts in cell layers of inner integuments and funiculus tissues (Figure 3O). Successful fertilization released this gradient, leading to a spreading of the *IAA9* transcript across the developing ovule at 3 DPA (Figure 3K).

Experimental Design for Combined Transcriptomic and Metabolomic Analysis of Fruit Set

In an attempt to identify important regulatory genes and metabolic pathways involved in tomato fruit set, we used transcriptomic and metabolomic approaches as well as real-time PCR analyses of target genes. The complete experimental design

included three parallel experiments (Figure 4). The first experiment aimed at defining the genes whose expression is associated with the transitions from bud through anthesis to the postanthesis stages and the corresponding metabolic shifts during natural fertilization-induced fruit set. The second experiment was designed to define the genes differentially expressed during pollination-independent fruit set in *AS-IAA9* plants. The third experiment aimed at identifying *IAA9* regulated genes (directly or indirectly regulated) during fruit set in ovary/fruit tissues. For this purpose, we conducted comprehensive analysis of gene expression in *AS-IAA9* and the wild type at three developmental stages during fruit set: flower bud, anthesis, and postanthesis. For each experiment, metabolomic changes associated with both types of fruit set were examined in wild-type and two independent *AS-IAA9* lines (Figure 4).

Oligonucleotide microarrays (EU-TOM1) containing 11,860 tomato unigenes were used to compare transcript profiles corresponding to preanthesis flower buds (−2 DPA), anthesis mature flower (0 DPA), and postanthesis fertilized flower (4 DPA) in the wild type and *AS-IAA9*. For each point, six Cy-labeled cDNAs corresponding to three independent biological samples with a dye-swap were hybridized to six independent array slides. The statistical analysis of the data was performed with R/MAANOVA package (see Methods).

General Feature of Fruit Set Expression Profiles

To identify new candidate genes that are essential for the fruit set process, we performed a comprehensive analysis of gene expression associated with the flower-to-fruit transition in wild-type pollination-dependent fruit set and in *AS-IAA9* pollination-independent fruit set. We compared the sets of differentially expressed genes between the two genotypes (Figure 5) and found, notably, that the overwhelming majority of the differentially expressed genes were common to both processes of fruit set (see Supplemental Table 4 online). In a further step, putative

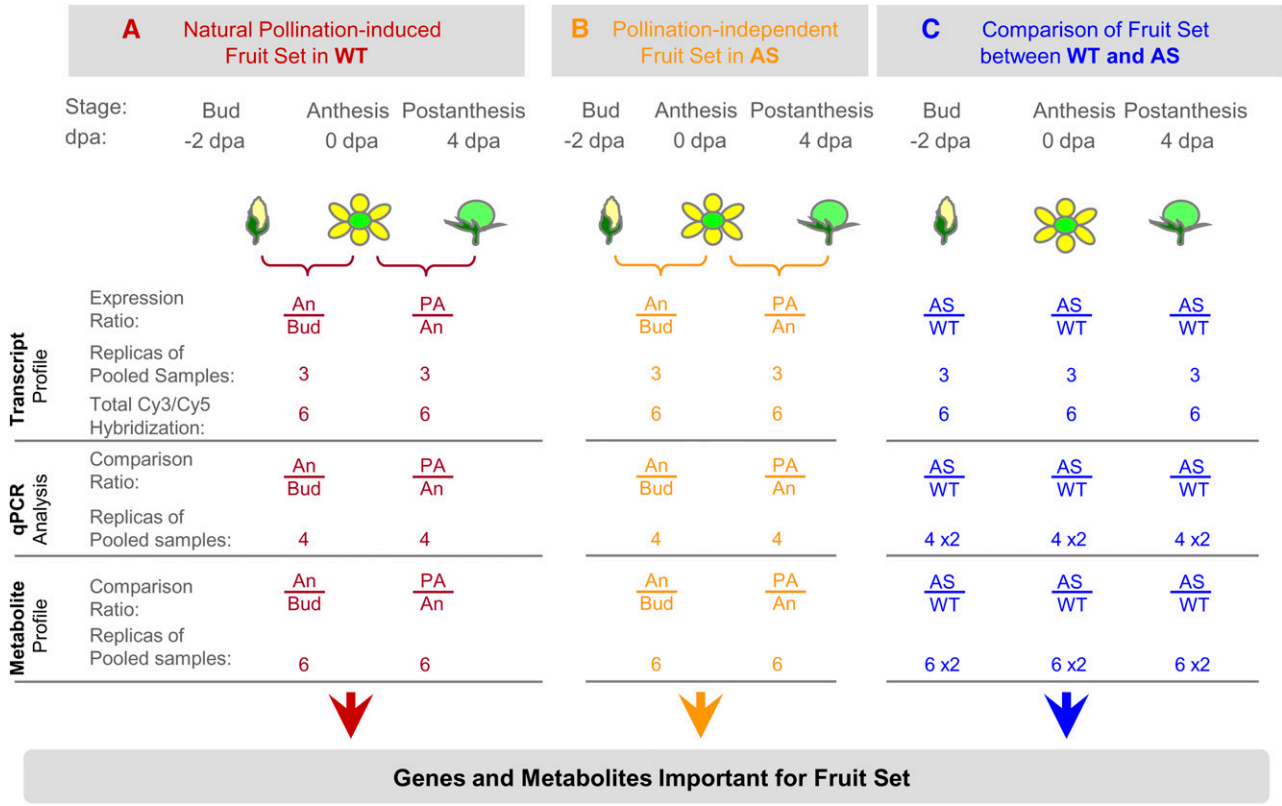

Figure 4. Experimental Design for Analyzing Transcriptomic and Metabolomic Changes Associated with Fruit Set in the Wild Type and *AS-IAA9*.

Combined transcriptomic and metabolomic approaches were used to investigate the molecular events associated with pollination-induced natural fruit set in the wild type **(A)**, pollination-independent fruit set in *AS-IAA9* (*AS*) **(B)**, and to identify differentially expressed genes or altered metabolites in antisense (AS) fertilization-free fruit set versus pollination-dependent fruit set in the wild type **(C)**. Bud (equivalent to 2 d before anthesis, −2 DPA), anthesis (An), and postanthesis (PA; 4 DPA) stages were considered. For transcriptome analyses, a direct comparison of *AS-IAA9* lines to their wild-type counterpart was employed. At each of the three developmental stages, Cy-labeled cDNAs were hybridized to six independent 12k-oligomicroarrays (EU-TOM1) using a triple dye-swap design. The abundance of a broad range of metabolites was quantified using GC-MS. Fruit/ovary tissues were pooled from wild-type (cv MicroTom) and *AS-IAA9* homozygous lines, and the samples were split into two parts, one to be used in microarray hybridization and the other in metabolite quantification. Cy3, cyanine3 fluor; Cy5, cyanine5 fluor; AS, *IAA9* antisense lines; qPCR, quantitative real-time PCR.

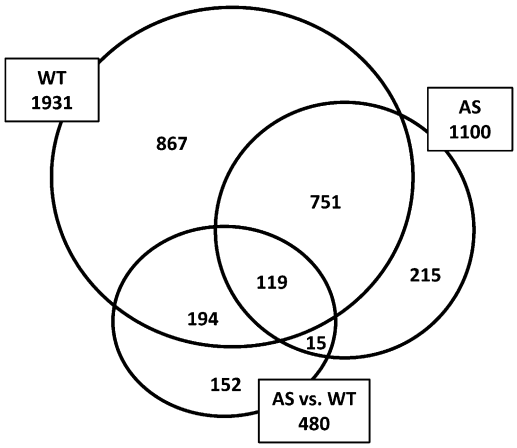

Figure 5. Venn Diagram of Fruit Set–Associated Genes.

Venn diagram showing genes differentially expressed during the three stages of flower-to-fruit transition in the wild type (red circle) and *AS-IAA9* (AS; yellow circle) tomato and differentially expressed between pollination-dependent and -independent fruit set (AS versus WT, blue circle). Overlap between each set of genes is indicated by different colors. Total numbers of differentially expressed genes are indicated in white boxes; the number of genes in each subset is indicated within the appropriate colored domain.

correlations between the genes that are differentially expressed during the transition from bud through anthesis to postanthesis in the wild type and *AS-IAA9* and those differentially expressed between the two genotypes were identified. In total, this study identified 870 genes (751 + 119) that are differentially expressed in both pollination-independent and pollination-dependent fruit set, among which only 119 display IAA9-dependent regulation (Figure 5; see Supplemental Table 5 online). Moreover, among the genes exhibiting differential expression during pollination-dependent fruit set (1931), the vast majority of genes were independent of IAA9 regulation. Similarly, among the genes that are common to both types of fruit set, the majority were independent of IAA9 regulation. This reflects the fact that only a small proportion of fruit set–associated genes is dependent on normal IAA9 regulation.

Transcriptome Analysis of Pollination-Induced Fruit Set in the Wild Type

Statistical analysis indicated that among 1931 differentially expressed genes in the wild type, 1455 genes exhibited differential expression during the transition from bud to anthesis stages and 1650 genes between anthesis and postanthesis stages (Figure 6; see Supplemental Table 1 online). The high number of genes displaying altered expression during fruit set is indicative of dynamic regulatory mechanisms underlying this developmental process. Functional categorization of the differentially expressed genes revealed that the major groups affected belong to gene categories encoding components of signal transduction, proteins involved in metabolic pathways, or proteins associated with cell division (Table 1). These results suggest that the fruit set process in tomato requires complex regulatory control and intensive cell division as well as reconfiguration of metabolic processes.

Surprisingly, the number of differentially regulated genes between bud and postanthesis was lower than during the transitions from bud to anthesis and from anthesis to postanthesis, consistent with a mechanism wherein a large number of genes undergo a transient up- or downregulation at the anthesis stage. Moreover, the majority of differentially expressed genes are downregulated during the transition from flower bud to anthesis, while the reverse occurs during the transition from anthesis to postanthesis (Figure 6A), indicating that there is no continuum of ovary development from bud to postanthesis.

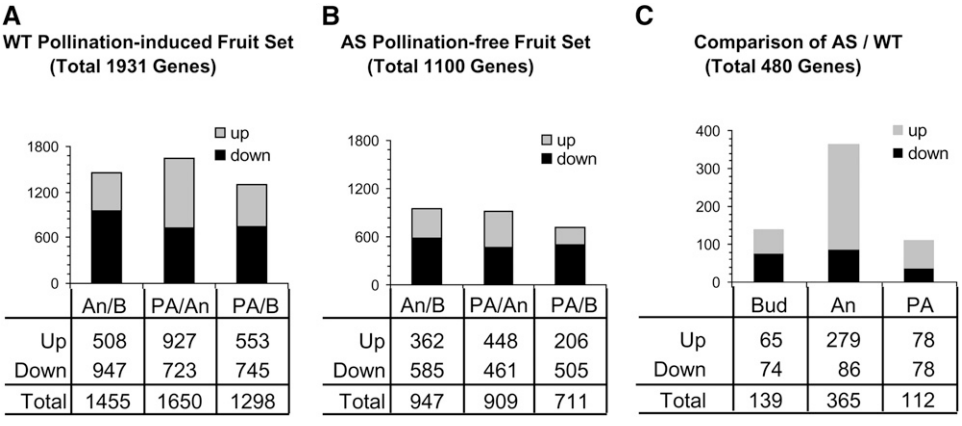

	An/B	PA/An	PA/B
Up	508	927	553
Down	947	723	745
Total	1455	1650	1298

	An/B	PA/An	PA/B
Up	362	448	206
Down	585	461	505
Total	947	909	711

	Bud	An	PA
Up	65	279	78
Down	74	86	78
Total	139	365	112

Figure 6. Global Gene Expression Pattern in Pollination-Dependent and -Independent Fruit Set.

(A) and **(B)** Differentially expressed genes (either up- or downregulated) during the transition from flower bud to anthesis and from anthesis to postanthesis in natural pollination-induced fruit set of wild-type plants **(A)** and pollination-free fruit set in antisense (AS) lines **(B)**.

(C) Differentially expressed genes between AS and the wild type during fruit set at three developmental stages: bud (B), anthesis (An), and postanthesis (PA). Upregulated (Up), downregulated (Down), and total altered genes (total) refer to changes in transcript accumulation displaying $\log_2$ (ratio) higher than 0.5 or lower than −0.5 (P value = 0.05).

Table 1. Functional Classification of Differentially Expressed Genes during Natural Pollinated Wild-Type Fruit Set

Assignment	An/B (Wild Type)		PA/An (Wild Type)		PA/B (Wild Type)	
	No. of Genes	%	No. of Genes	%	No. of Genes	%
Hormone responses	67	5	75	5	61	5
Signal transduction[a]	349	24	365	22	295	23
Metabolism	286	20	357	22	269	21
Cell division	116	8	161	10	136	10
Photosynthesis	52	4	54	3	37	3
Cell wall	39	3	45	3	36	3
Cell structure	24	2	29	2	16	1
Stress/defense responses	97	7	100	6	85	7
Transporter	72	5	92	6	73	6
Others	38	3	44	3	43	3
Unknown	315	22	328	20	247	19
Total	1455	100	1650	100	1298	100

[a]Including transcription factor.

Transcriptome Analysis of Fertilization-Independent Fruit Set in *AS-IAA9*

Statistical analysis of the global gene expression associated with pollination-independent fruit set in *AS-IAA9* indicated that 947 genes exhibited differential expression during the transition from bud to anthesis (Figure 6B; see Supplemental Table 2 online) and 909 from anthesis to postanthesis (Figure 6B). In contrast with pollination-induced fruit set where the highest transition occurs between anthesis and postanthesis, the major shift in terms of change in transcript accumulation in *AS-IAA9* occurs at the transition from bud to anthesis.

Functional categorization of the differentially expressed genes (Table 2) revealed that the major groups affected during the process of fruit set in antisense lines belong to gene categories encoding components of signal transduction, metabolic pathways, and cell division. Of particular note, the percentage of cell division–associated genes changing on the developmental transition is considerably lower in *AS-IAA9* compared with that found in the wild type.

Comparative Transcriptome Analysis of Wild-Type and *AS-IAA9* Fruit Set

We next sought to identify genes that are differentially expressed between the two genotypes during fruit set. When all three developmental stages are considered, a total of 480 genes showed differential expression between wild-type and *AS-IAA9* lines (Figure 5), and the difference between the two lines was greatest at anthesis (Figure 6C). Functional classification of these differentially expressed genes (Table 3) revealed that the major discriminating factors between the two lines are dependent on the developmental stage. That is, at flower bud stage, the major groups of differential genes belong to the category of signal transduction, whereas at anthesis stage, the most prevalent groups encode proteins involved in cell division and metabolism. At postanthesis stage, the most discriminating groups are those associated with photosynthesis (35%) and metabolism. Functional classification of these genes (Table 3) also indicates that among the differentially expressed genes, those exhibiting potential regulatory function (such as those involved in hormone response or signal transduction) decrease steadily from bud to postanthesis stage, while those associated with potential executor function (such as those involved in photosynthesis, cell division, and metabolism), increase from bud to postanthesis.

Validation of Microarray Expression Data by Quantitative RT-PCR

Quantitative real-time-PCR (qRT-PCR) was used to validate the microarray analysis data and to further define the expression pattern of selected genes, relating to our biological focus, during fruit set. Representatives from 11 functional groups of differentially expressed genes between *AS-IAA9* and the wild type (Table 1) were selected for qRT-PCR. In total, 25 genes were analyzed and the resultant qRT-PCR profiles were compared with microarray expression profiles and scored as matching if they agreed in the expression pattern. By this criterion, 90% of the values have the same pattern of expression in the microarray experiment as in the qRT-PCR experiment, whereas for the remaining 10%, only one or two biological repetition out of four showed the same pattern of expression in the microarray experiment (see Supplemental Table 7 online).

Downregulation of *IAA9* Strongly Promotes Photosynthesis-Related Genes at Fruit Set

During pollination-induced fruit set, photosynthesis-related genes were downregulated during the transition from bud to anthesis, whereas they were generally upregulated from anthesis to postanthesis (see Supplemental Table 1 online). By contrast, photosynthesis-related genes were strongly activated in *AS-IAA9* throughout fruit set (Table 3), and, notably, all these genes without exception (43 in total) were upregulated in the *AS-IAA9*

Table 2. Functional Classification of Differentially Expressed Genes during Pollinated-Independent Fruit Set in *AS-IAA9* Lines

Assignment	An/B (AS)		PA/An (AS)		PA/B (AS)	
	No. of Genes	%	No. of Genes	%	No. of Genes	%
Hormone responses	50	5	48	5	39	5
Signal transduction[a]	242	26	212	23	170	24
Metabolism	180	19	190	21	135	19
Cell division	54	6	50	6	42	6
Photosynthesis	26	3	28	3	25	4
Cell wall	23	2	24	3	20	3
Cell structure	18	2	17	2	14	2
Stress/defense responses	66	7	59	6	55	8
Transporter	53	6	55	6	42	6
Others	22	2	24	3	22	3
Unknown	213	22	202	22	147	21
Total	947	100	909	100	711	100

[a]Including transcription factor.

Table 3. Functional Classification of Differentially Expressed Genes between Antisense and the Wild Type during Fruit Set

	Bud (AS versus WT)		An (AS versus WT)		PA (AS versus WT)	
Assignment	No. of Genes	%	No. of Genes	%	No. of Genes	%
Hormone responses	16	12	17	5	4	4
Signal transduction[a]	23	17	36	10	11	10
Metabolism	21	15	74	20	22	20
Cell division	22	16	108	30	13	12
Photosynthesis	2	1	29	8	39	35
Cell wall	7	5	18	5	2	2
Cell structure	1	1	8	2	5	4
Stress/defense responses	19	14	27	7	8	7
Transporter	8	6	14	4	2	2
Others	4	3	11	3	0	0
Unknown	16	12	23	6	6	5
Total	139	100	365	100	112	100

[a]Including transcription factor.

lines compared with the wild type (see Supplemental Table 3 online). qRT-PCR analysis (Figures 7A and 7B) further confirmed the expression profile revealed by microarray for two photosynthesis-associated genes encoding chlorophyll *a*/*b* binding protein 4 (*CAB4*) and chlorophyll *a*/*b* binding protein 1D (*CAB-1D*). The two genes were upregulated at postanthesis stages in the wild type, and their upregulation continued during subsequent cell division and enlargement phases of fruit development (Figure 7C). In line with the upregulation of photosynthesis-related genes, downregulation of *IAA9* was associated with a dramatic upregulation of genes involved in sucrose catabolism (Figure 7D), particularly at the postanthesis stage and to a lesser extent at the anthesis stage, suggesting the importance of these genes in the processes of the flower-to-fruit transition. Notably, all sugar metabolism genes that are differentially expressed between *AS-IAA9* and the wild type displayed upregulation during the fruit set developmental process, suggesting that activation of sugar metabolism may be an important event coupled with the initiation of pollination-independent fruit set.

The Fruit Set Process Recruits a High Number of Transcriptional Regulators

Up to 199 transcription factors displayed differential expression during natural fruit set. Such a high number of transcriptional regulators is indicative of the massive and complex regulation required for the fruit set process (see Supplemental Table 1 online). Comparing the transcriptomic profiles associated with the fruit set process in the wild type and *AS-IAA9* revealed that 18 transcription factors showed differential expression between the two genotypes (see Supplemental Table 3 online). qRT-PCR analysis showed that during natural pollination-induced fruit set in the wild type, the expression of two MADS box genes, *Tomato Agamous1* (*TAG1*) and *Tomato Agamous-like 6* (*TAGL6*), underwent dramatic downregulation following fertilization exhibiting seven- and eightfold decreases in the level of transcript accumulation, respectively (Figure 8A). Interestingly, during later stages of fruit development, the expression level of the two genes continued to display sharp and steady decreases with *TAG1* and *TAGL6* transcripts dropping at 10 DPA to ~10 and 1% of their levels at 1 DPA, respectively (Figure 8C). Moreover, compared with the wild type, the two MADS box genes underwent a net downregulation during fruit set in *AS-IAA9* lines, which was most prominent at the anthesis stage (Figure 8B). Since both natural and pollination-independent fruit set were both characterized by a net downregulation of *TAG1* and *TAGL6*, it can be speculated that these two MADS box genes are key players in the process of fruit set and that *AS-IAA9* may promote fertilization-independent fruit set by downregulating their expression.

Upregulation of Cell Division-Related Genes Is Advanced in *AS-IAA9* Lines

A number of cell division, protein biosynthesis, and cell wall–related genes were upregulated at the postanthesis stage in the wild type, while their activation occurred earlier in *AS-IAA9* at the anthesis stage (see Supplemental Tables 1 and 2 online). Remarkably, when comparing pollination-dependent and -independent fruit set, these genes were found to be upregulated in *AS-IAA9* at the anthesis stage but downregulated at postanthesis (see Supplemental Table 3 online). These included *cyclinA3*, *cyclinb*, and 19 unigenes coding for histones that all displayed higher expression in *AS-IAA9* at anthesis stage. A large group of 67 ribosomal protein genes was also all upregulated at anthesis stage in *AS-IAA9*. A total of 24 cell wall–related genes were differentially expressed in *AS-IAA9*, with a large majority of them being upregulated, including *cellulose synthases*, *expansins*, *extensins*, *polygalacturonase*, and *glucanases*. In particular, the polygalacturonase inhibitor protein (*PGIP1*) gene, putatively involved in fruit enlargement, was very strongly upregulated (sevenfold) at both bud and anthesis stages in *AS-IAA9*, but only at postanthesis in naturally pollinated wild-type young fruit (see Supplemental Tables 1 and 3 online).

The expression of two histone protein genes and two ribosomal protein genes during the flower-to-fruit transition in wild-type lines displayed a strong activation at 4 DPA (Figure 9A) and then a sharp decline after 10 DPA, coinciding with the shift from cell division to cell enlargement phases (Figure 9C). Interestingly, the upregulation of these genes occurred at anthesis stage in *AS-IAA9.* Consistently, when compared with the wild type, the expression of all four genes was upregulated in *AS-IAA9* at both bud and anthesis stages but was clearly downregulated at the postanthesis stage (Figure 9B). By contrast, the *expansin10* gene showed higher expression in *AS-IAA9* compared with the wild type throughout the three stages of fruit set, and its transcript levels remained high after the shift from cell division to fruit enlargement during natural fruit development (Figures 9B and 9C).

Expression of Phytohormone-Related Genes during the Process of Fruit Set

Taking into account the prominent role played by phytohormones in triggering and coordinating the flower-to-fruit transition

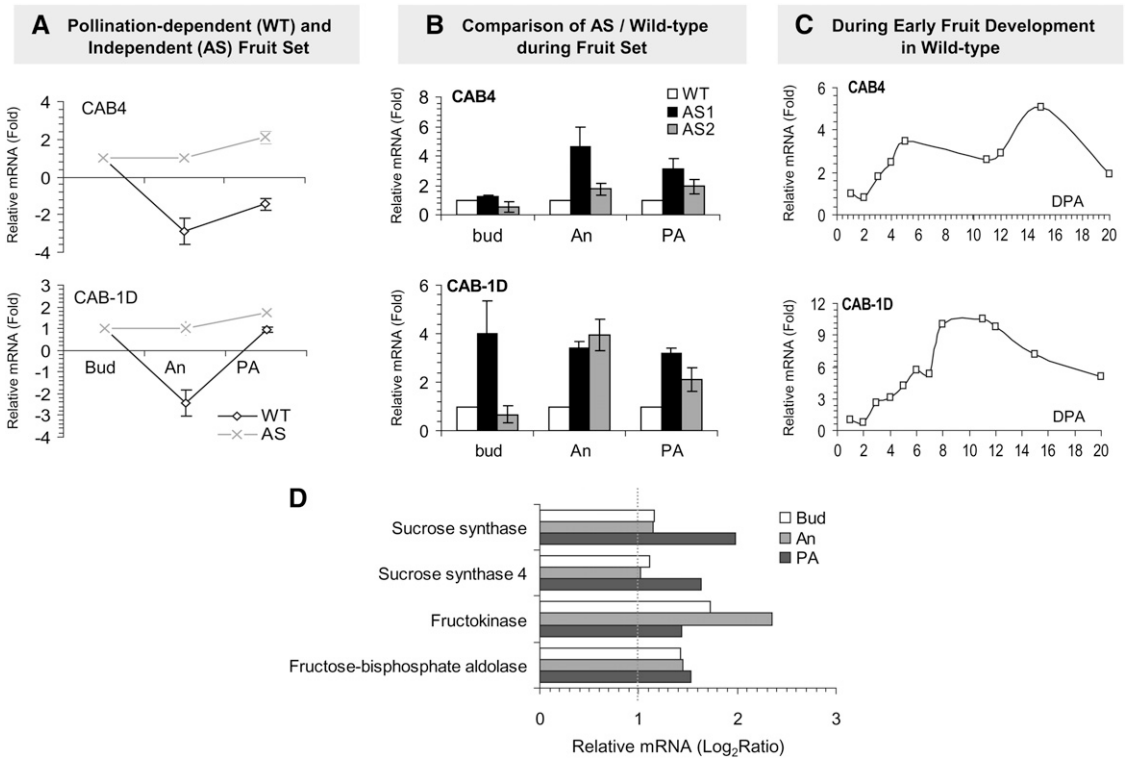

Figure 7. Expression Analysis of Genes Involved in Photosynthetic Processes and Sugar Metabolism.

(A) Expression kinetics of selected photosynthetic genes during pollination-dependent fruit set in wild-type (black line) and pollination-free fruit set in *AS-IAA9* (gray line) assessed by qRT-PCR. cDNA were prepared from the same RNA samples used in the microarray experiment. Data are expressed as relative values, based on the values of bud ovary taken as reference sample set to 1.

(B) Comparison of transcript levels between the wild type (white bar) and two independent *AS-IAA9* lines *AS1* (black bar) and *AS2* (gray bar) assessed by qRT-PCR at three developmental stages. Data are expressed as relative values, based on the reference wild-type samples set to 1.0 at each stage considered.

(C) Transcript accumulation during early stage of natural pollination-induced fruit set in the wild type. Relative expression levels for stages 2 to 20 DPA were determined based on the reference 1 DPA sample set to 1.0. CAB4, *chlorophyll a/b binding protein 4*; CAB-1D, *chlorophyll a/b Binding Protein1D*. Error bars represent ± SE of four biological repetitions.

(D) Comparative transcript accumulation in the wild type at different stages of genes involved in sugar metabolism identified by microarray analysis as differentially expressed between wild-type and antisense lines.

developmental process, we closely examined transcript accumulation of genes associated with hormone responses and metabolism. During natural pollinated fruit set, almost 5% of the differentially expressed genes was related to hormone metabolism and signaling (Table 1). Functional category classification of these genes indicated that auxin, ethylene, and polyamine-associated genes were the most prominent in this developmental process (Figure 10A, left panel) as well as in the pollination-free fruit set of *AS-IAA9* (Figure 10A, right panel). The high number of ethylene-related genes observed to change suggests that in addition to the well-established role of auxin and GAs (Pandolfini et al., 2007; Serrani et al., 2007), ethylene must also play an active role in fruit set. Detailed evaluation of the ethylene-associated genes reveals that they included both key ethylene signal transduction pathway and ethylene biosynthesis genes (see Supplemental Table 1 online).

qRT-PCR analysis (Figures 10B to 10D) indicated that, in both the wild type and *AS-IAA9*, the expression of all hormone-related genes selected underwent dramatic downregulation following the anthesis stage (Figures 10B to 10D, left panel), which continued until at least 14 DPA in the wild type (Figures 10B to and 10D, right panel). Notably, the downregulation of auxin-related genes occurred earlier (2 DPA) than that of ethylene-related genes (6 DPA). As a general feature, the hormone-related genes displayed lower expression in *AS-IAA9* lines compared with the wild type (Figures 10B to 10D, middle panel). According to these data, auxin and ethylene are the two hormones most prominently involved in the control of the flower-to-fruit transition developmental process.

Aux/IAA and *ARF* Genes Are Strongly Regulated during Fruit Set

Considering the role of IAA9 in mediating auxin responses and that generally ascribed to auxin in the process of fruit set, we sought to study the expression profile of all members of the *Aux/*

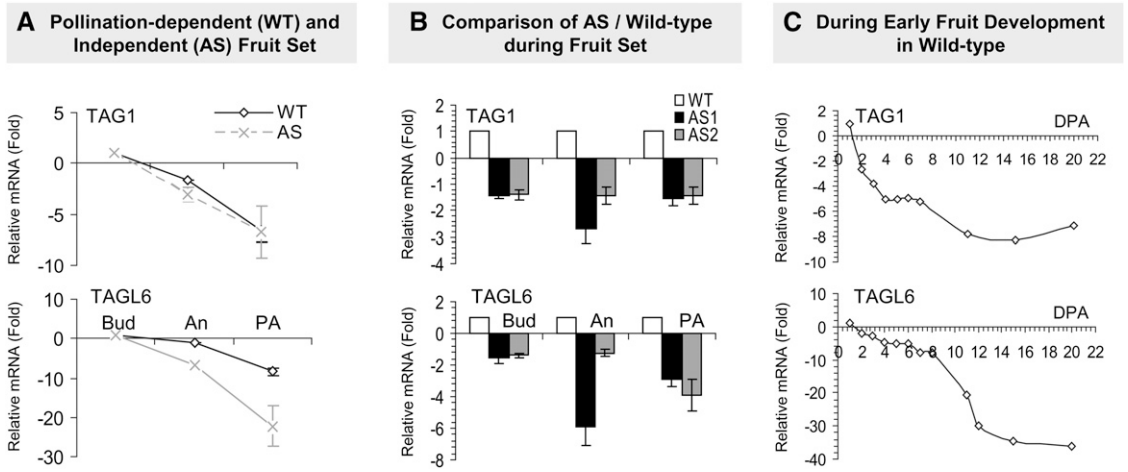

Figure 8. Expression Analysis of Two MADS Box Genes Assessed by qRT-PCR.

(A) Expression kinetics of two MADS box genes (*TAG1* and *TAGL6*) during pollination-dependent (wild-type, black line) and pollination-free (*AS-IAA9*, gray line) fruit set. Data are expressed as relative values based on bud ovary taken as reference sample set to 1.0.

(B) Comparison of transcript levels between wild-type (white bar) and two independent *AS-IAA9* lines *AS1* (black bar) and *AS2* (gray bar) at three developmental stages. Data are expressed as relative values, based on the reference wild-type samples set to 1.0.

(C) Transcript accumulation during early stage of natural pollination-induced fruit set in the wild type. Relative expression levels for stages 2 to 20 DPA were determined based on the reference value of 1 DPA sample set to 1.0. TAG1, *Tomato Agamous 1*; TAGL6, *Tomato Agamous-like6*. Error bars represent ± SE of four biological repetitions.

IAA and auxin transcription factors (*ARF*) gene families available in tomato. The expression data (Figure 11) indicate that throughout the process of natural fruit set, both *ARFs* and *Aux*/*IAAs* display a dramatic shift in their expression, suggesting an active role of these transcriptional regulators in this developmental process. Moreover, downregulation of *IAA9* resulted in a feedback regulation of a number of *ARF* and *Aux*/*IAA* genes. Of particular note is the fact that half of the *ARF* genes tested (7 out of 14) undergo opposite regulation during the transitions from bud to anthesis and from anthesis to postanthesis (Figure 11A). The expression of the overwhelming majority of *ARF* genes at the bud stage was strongly upregulated in *AS-IAA9* lines compared with the wild type (Figure 11B). Notably, *ARF4*, *ARF8*, and *ARF18* showed strong upregulation upon pollination in the wild type, and their expression levels were higher in the *AS-IAA9* line at bud stage, suggesting their potential involvement in the process of pollination-independent fruit set. Most *Aux*/*IAA* genes (13 out of 18) were downregulated during the transition from bud to anthesis, whereas a number of them (six genes) displayed clear upregulation during the transition from anthesis to postanthesis. The *Aux*/*IAAs* genes that were upregulated upon pollination in the wild type (*IAA1*, *IAA3*, *IAA11*, *IAA13*, *IAA14*, and *IAA30*) displayed higher expression in *AS-IAA9* than in wild-type lines at bud stage, suggesting that the upregulation of these genes is integral to the fruit set process.

Metabolite Accumulation in Ovary/Fruit during Natural Pollinated Fruit Set

Information related to metabolic changes underlying the flower-to-fruit transition are still lacking, and the studies of flower metabolism in various species generally tend to be confined to specific pathways of importance with respect to color or fragrance (Dudareva et al., 1996; Moyano et al., 1996; Dunphy, 2006). To identify the changes in primary metabolism that underlie the flower-to-fruit transition, an established gas chromatography–mass spectrometry (GC-MS) method was applied to extracts from the materials described in the experimental design (Figure 4). Comparing the metabolite contents between the samples harvested at anthesis and bud stages in the wild type revealed little difference in the metabolism of these developmental stages. By contrast, many changes were observed between the samples harvested at anthesis and postanthesis. The differences detected are summarized in Figure 12 (while the absolute values are presented in Supplemental Table 6 online). In the wild type, differences observed between bud and anthesis stages were confined to increases in raffinose, glycerol 3-phosphate, fructose 6-phosphate, Val, Phe, Tyr, and His and a decrease in the level of galactonate-1,4-lactone (Figure 11, white bars). When comparing anthesis and postanthesis stages, a total of 22 of the 73 compounds measured were found at significantly different levels (see Supplemental Table 6 online). In a few instances, the direction of these changes was reversed from that observed between bud and anthesis. Raffinose, mannose, L-ascorbate, glucose-6-phosphate, maltitol, glycerol-3-phosphate, Leu, Val, Ala, Phe, Trp, isocitrate, Gln, Arg, and putrescine all significantly decrease at postanthesis to values as low as those recorded at the bud stage (see Supplemental Table 6 online). By contrast, few increases in metabolite level were observed with galactonate-1,4-lactone, gluconate-1,5-lactone, threonate, pyruvate, Asp, and 5-oxoproline being markedly elevated at this time point.

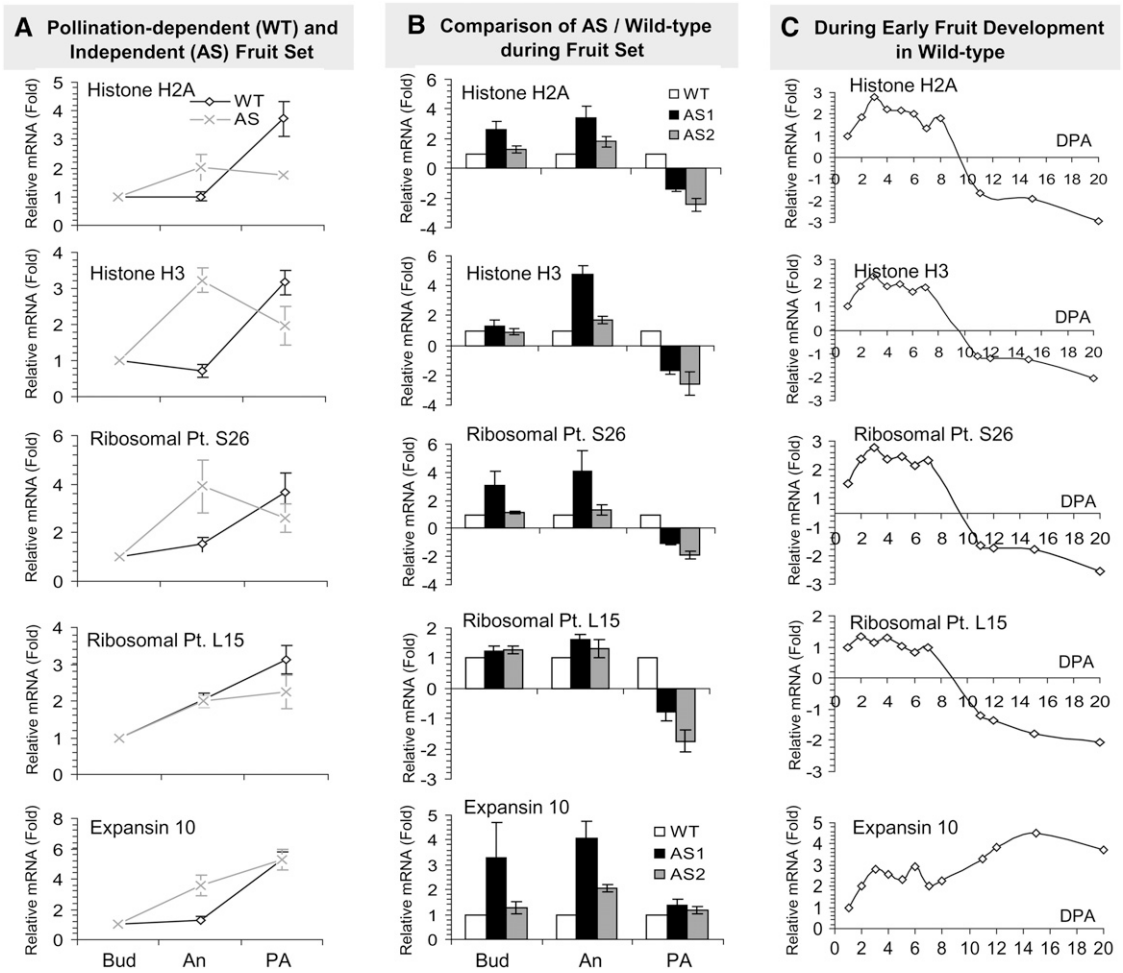

Figure 9. Expression Analysis of Cell Division–Related Genes Assessed by qRT-PCR.

(A) Expression kinetics of two histone genes (*Histone H2A* and *Histone H3*), two ribosomal protein genes (*Ribosomal Pt. S26* and *Ribosomal Pt. L15*), and *Expansin 10* gene during pollination-dependent (wild-type, black line) and pollination-free (*AS-IAA9*; gray line) fruit set. Data are expressed as relative values, based on bud ovary taken as reference sample set to 1.

(B) Comparison of transcript levels between wild-type (white bar) and two independent *AS-IAA9* lines *AS1* (black bar) and *AS2* (gray bar) at three developmental stages. Data are expressed as relative values, based on the reference wild-type sample set to 1.0.

(C) Transcript accumulation during early stage of natural pollination-induced fruit set in the wild type. Relative expression levels for stages 2 to 20 DPA were determined based on the reference 1 DPA sample set to 1.0. Error bars represent ± SE of four biological repetitions.

Metabolite Accumulation in Ovary/Fruit Revealed Considerable Differences between Fertilization-Dependent and -Independent Fruit Set

The scale of change in metabolite contents between the floral bud and anthesis samples was dramatically enhanced in the transgenic lines (Figure 12, gray bars). These changes included increased levels of glucose, fructose, sucrose, xylose, inositol, gluconate-1,5-lactone, galactonate-1,4-lactone, ribose-5-phosphate, amino acids derived from pyruvate (Leu, Ile, and Ala), oxaloacetate (Asp, Asn, and Lys), and 2-oxoglutarate (Glu and Gln), as well as increased levels of Gly, threonate, and citrate at the anthesis stage. In addition, the shikimate pathway was upregulated in the antisense lines, as evidenced by the higher levels of both Tyr and the large increase in shikimate itself (Figure 12, gray bars; see Supplemental Table 6 online). The transgenic genotype also displayed large changes with many metabolites returning to levels comparable to those observed at the bud stage. Particularly dramatic changes in the levels of fructose, glucose, inositol, citrate, glycerol 3-phosphate, fructose 6-phosphate, Ala, Asn, Glu, Leu, Tyr, and shikimate can be seen in Figure 12 (gray bars). These combined changes indicate that far fewer of the metabolites displayed significant differences at postanthesis stage in comparison to the control (bud stage).

Fertilization-independent fruit set is characterized by a massive increase in sugars and sugar derivatives at the anthesis stage, with fructose, glucose, sucrose, inositol, and trehalose all being dramatically increased. However, the levels of glucose, inositol, and trehalose fell substantially at subsequent stages.

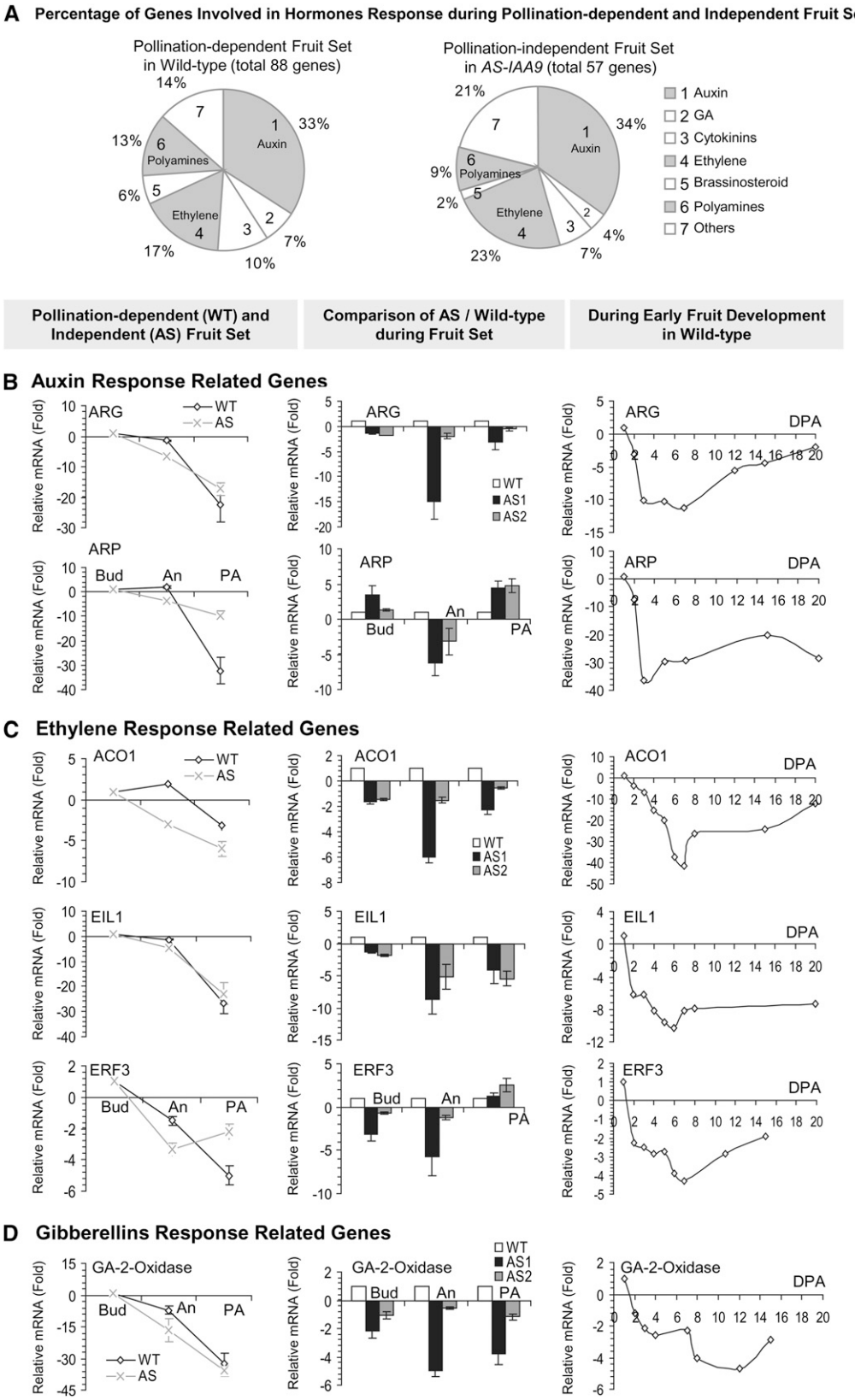

Figure 10. Expression Analysis of Hormone-Related Genes.

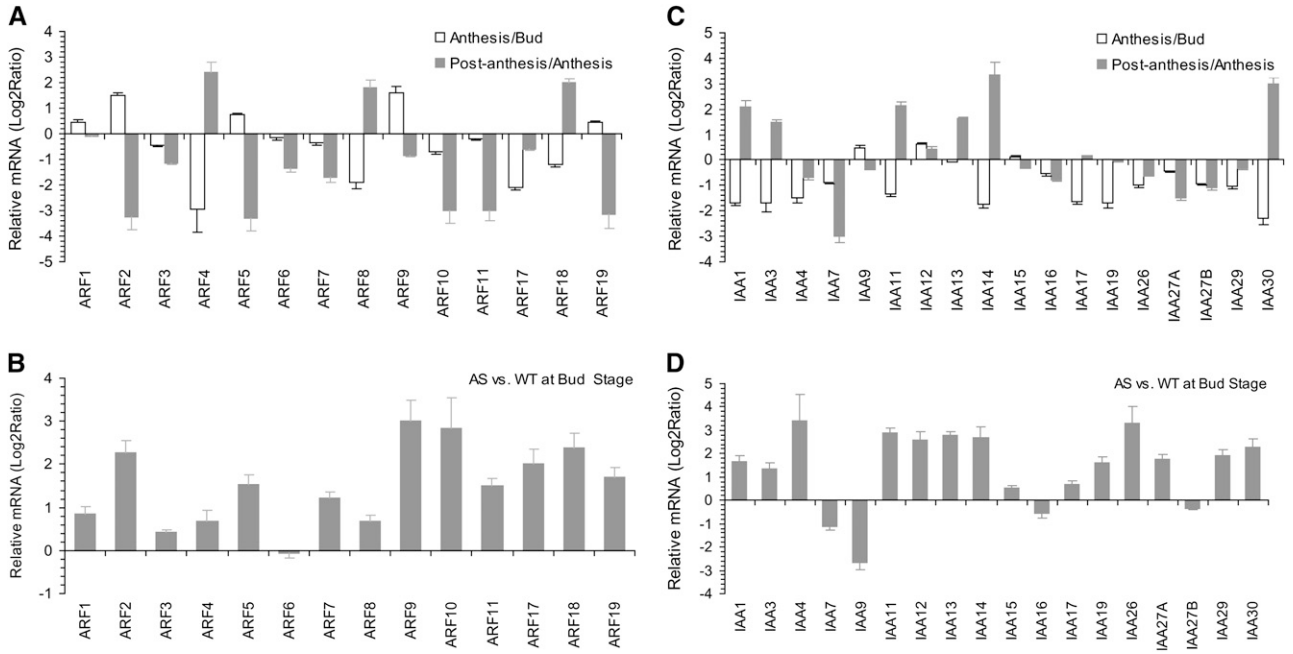

Figure 11. Expression Profile of Auxin Response Transcription Factors during Fruit Set.

(A) and **(C)** Expression profile of *ARF* **(A)** and *Aux/IAA* **(C)** during pollination-induced fruit set in wild-type lines. Data are expressed as relative values, white bars indicate the relative transcripts level in anthesis stage compared with bud stage, and dark-gray bars indicate level in postanthesis stage compared with anthesis stage.

(B) and **(D)** Expression profile of *ARFs* **(B)** and *Aux/IAAs* **(D)** in *AS-IAA9* pollination-free fruit set lines. Data are expressed as relative values, which indicate the relative transcript levels in *AS-IAA9* lines compared with the wild type at bud stage. Expression analysis was assessed by real-time PCR, and data are expressed as relative value $\log_2$ ratio.

Interestingly, this effect is not mirrored by the levels of fructose 6-phosphate or glycerol 3-phosphate, which exhibited similar dynamic behavior across development in both types of fruit set. Organic acids were also generally present at higher levels throughout development during fertilization-independent fruit set. Notably, citrate was at significantly higher levels in the transgenics during anthesis, as was the ascorbate precursor galactonate-1, 4-lactone; however, both compounds returned to levels observed in the wild type by 4 DPA. Consistent changes in the levels of some amino acids were also observed (Figure 12, black bars). Ala is present at considerably higher levels at both anthesis and postanthesis stages in the transgenic lines, as is Leu, perhaps indicating a higher metabolic rate associated with fertilization-independent fruit set. Glu and Gln as well as Tyr and shikimate are all at significantly enhanced levels in the *AS-IAA9* lines at the bud stage. In addition, the levels of Trp are clearly decreased at all three developmental stages, perhaps indicating an important role for this metabolite in fertilization-dependent fruit set.

Integration of Metabolite and Transcript Profiling Data Obtained during Pollination-Dependent Fruit Set

Given that the determination of metabolite and transcript levels were performed in the exact same samples, we then investigated whether further biological insights were accessible following

Figure 10. (continued).

(A) Expression of hormone-related genes differentially expressed during pollination-dependent fruit set in the wild type (left panel) and pollination-free fruit set in *AS-IAA9* (right panel). The most prominent groups are shaded gray. The category called "Others" includes abscisic acid, jamonic acid, and salicylic acid.

(B) to **(D)** Expression analysis assessed by qRT-PCR of auxin response-related genes **(B)**, ethylene response-related genes **(C)**, and GA response-related genes **(D)**. Left panel, expression kinetics of selected hormone-related genes during pollination-dependent fruit set in the wild type (black line) and pollination-free fruit set in *AS-IAA9* (gray line); data are expressed as relative values, based on the reference bud ovary sample set to 1.0. Middle panel, comparison of transcript levels between wild-type (white bar) and two independent *AS-IAA9* lines *AS1* (black bar) and *AS2* (gray bar) at three developmental stages. Data are expressed as relative values, based on the reference wild-type samples set to 1.0. Right panel, transcript accumulation during early stage of natural pollination-induced fruit set in the wild type. Relative expression levels for stages 2 to 20 DPA were determined based on the reference 1 DPA sample set to 1.0. ARG, auxin-repressed gene; ARP, auxin-regulated gene; ACO1, ACC oxidase1. Error bars represent ± SE of four biological repetitions.

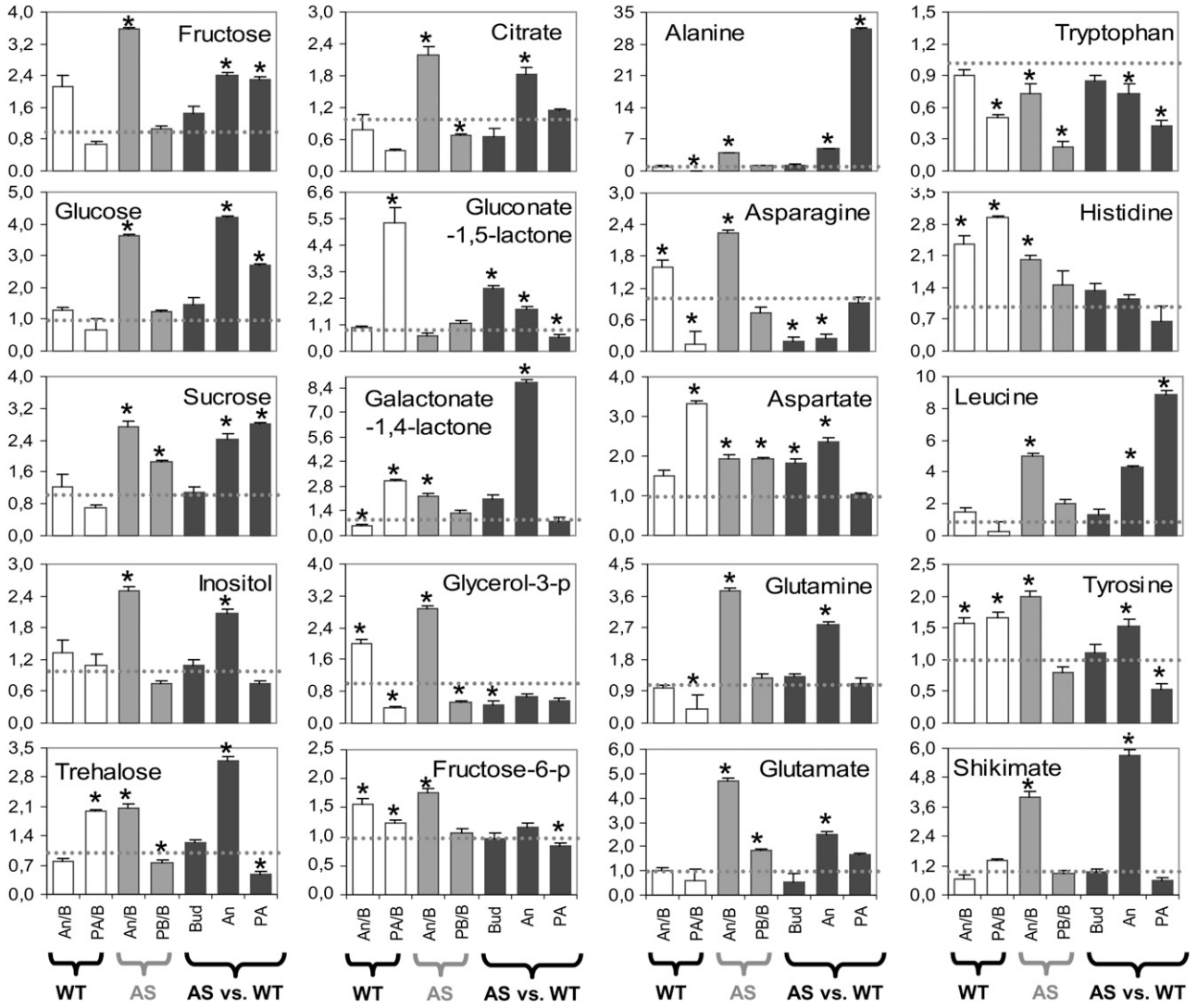

Figure 12. Comparative Analyses of Metabolic Changes Associated with Pollination-Dependent and -Independent Fruit Set.

White bars represent metabolic changes during pollination-dependent fruit set in the wild type. The relative metabolite level of anthesis (An/B) and postanthesis (PA/B) were determined compared with that of wild-type flower bud, which was set to 1.0. Gray bars show the metabolic change during pollination-independent fruit set in *AS-IAA9*. The relative metabolite level of anthesis and postanthesis were determined compared with that of *AS-IAA9* flower bud, which was set to 1.0. Black bars present changes in the metabolite profile in antisense line AS1 compared with wild-type lines during flower-to-fruit transition at three different developmental stages of bud, An (anthesis), and PA (postanthesis). The relative metabolite level was determined compared with that of the wild type at each stage. The dotted lines in the diagrams reflect the normalized control (1.0). The changes are represented as means ± SE of determinations of six individual pooled samples. An asterisk indicates changes deemed by the Student's *t* test ($P < 0.05$) to be statistically significant.

integration of these data using two different approaches. First, we uploaded the combined data sets into the MapMan software framework to allow full access to our data for further interrogation (http://mapman.mpimp-golm.mpg.de/supplement/wang/). A visualization of the connectivity between functionally classified transcripts and metabolites can be seen in the PageMan (Usadel et al., 2005) representation of Figure 13. To comprehensively investigate this, we compared changes in either the wild type (Figure 13A), the *IAA9* antisense lines (Figure 13B), or the ratios between the two genotypes during each transition and across the whole developmental process (Figure 13C). Interestingly, given that there were proportionally far more changes in the levels of metabolites than transcripts, the general picture is that most metabolite levels do not seem to be directly related to the levels of transcripts associated with their metabolism. However, certain observations, such as the similar trend in the levels of transcripts associated with photosynthesis and the levels of major carbohydrates, suggest that regulatory modules can be

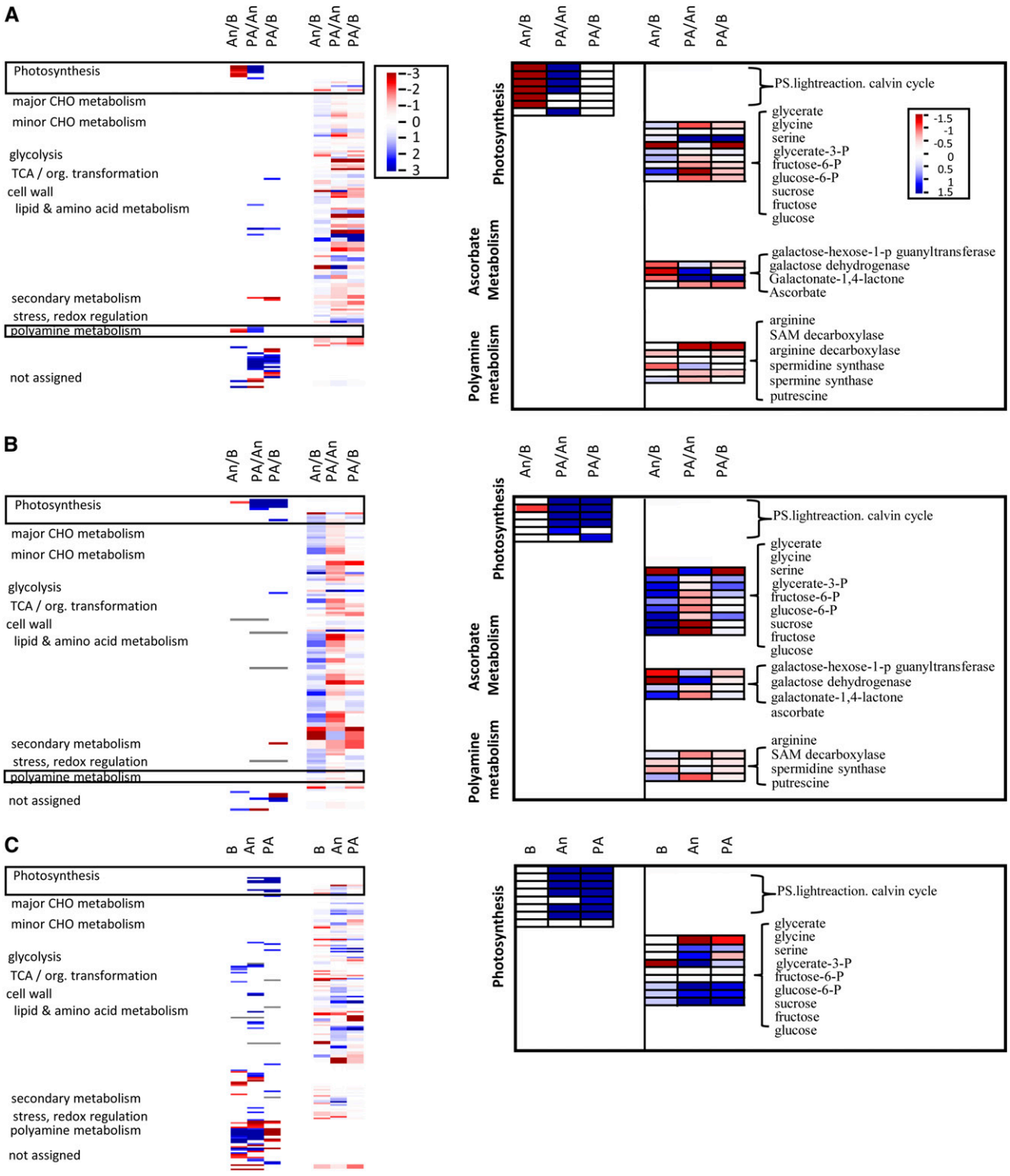

Figure 13. Integrated Analysis of Transcriptional and Metabolic Changes.

The left-hand side the figure shows the color-coded results of a Wilcoxon test for a consistent upregulation (blue) or downregulation (red) of individual processes for the whole data set (columns 1 to 3). Average levels of metabolites as well as averages of metabolites per process are also color coded in the same manner (columns 4 to 6). In the panel on the right-hand side, individual processes are magnified, and processes or metabolites are labeled individually. The results of the Wilcoxon test are shown in the first columns. The next columns show individual metabolites or the averages of individual enzyme classes. Processes or enzyme classes not flagged as significant have been omitted for clarity. The three independent graphs represent changes in the wild type **(A)**, *IAA9* antisense line **(B)**, and the comparison of these genotypes obtained by dividing the $\log_2$ transformed values of the antisense by similarly transformed values of the wild type **(C)**.

identified within the data set (Figure 13A). By contrast, the *IAA9* antisense line displayed clearer correlative changes between transcript and metabolite levels with strong upregulation of transcripts associated with both the photosynthetic apparatus and enzymes of the Calvin cycle.

To further explore correlative changes between metabolites and transcripts, we performed a manual consistency check between those metabolites that display differences in abundance and transcripts associated to the corresponding metabolic pathways (http://mapman.mpimp-golm.mpg.de/supplement/wang/). There were many cases in which the changes in metabolites were, at least partially, reflected by changes in the levels of transcripts associated with either their synthesis or degradation. The levels of His, Ala, and Asp provide good examples of such instances (see Supplemental Figures 1 to 3 online). Changes in the levels of His (which increased) were similar to those observed in the transcript level of histidinol-phosphate aminotransferase. In addition, changes documented in Ala levels were similar to those for the transcript levels of Ala glycoxylate transferase. Similarly, Asp displayed a similar upregulation as was observed in one of the isoforms of Asp aminotransferase (see online pathway visualizations and supplemental data for details). In two occasions, further potential transcriptional pathway regulation became apparent following the application of consistency analysis. The first of these is in the pathway of polyamine biosynthesis; at the anthesis stage, several S-adenosylmethionine (SAM) decarboxylases as well as several spermidine synthases were downregulated. However, the levels of the spermidine synthase genes were upregulated again in the postanthesis stage, which might explain the lowered levels of putrescine found during this stage. This metabolite is potentially depleted by its flux into spermidine (Figure 13A, right panel), which is in keeping with previous reports of a rise of free spermidine and spermine levels during early tomato fruit development (Egea-Cortines et al., 1993). Furthermore, a depletion of Arg was also identified, which feeds into the polyamine biosynthesis pathway through Arg decarboxylase. The identification of transcriptional control of this pathway also may explain its identification as an overrepresented functional category. Secondly, the ascorbate pathway exhibited similar behavior (Figure 13A, right panel). While, ascorbate levels fell during the transition from anthesis to the postanthesis stage, the levels of its direct precursor, galactonate 1,4-lactone, conversely decreased during anthesis before rising again at postanthesis. Interestingly, the transcript levels of both galactose-dehydrogenase (L-Gal-DH) and GDP-L-galactose-hexose-1-phosphate guanyltransferase were repressed during the anthesis stage with L-Gal-DH recovering during postanthesis and was thus able to account for the change in levels of galactonate 1,4-lactone. Furthermore, several transcripts coding for enzymes potentially involved in the production of glucuronate (an alternative precursor for ascorbate) were upregulated at later developmental stages.

By contrast, there was no correlation between transcript and metabolite changes for some of the metabolites displaying change throughout the fruit set process, such as raffinose and Leu, no consistent transcript responses could be detected, indicating that these metabolites are unlikely to be controlled at the transcriptional level. However, it is important to note that caution must be taken when interpreting these data since the EU-TOM1 does not offer genome-wide coverage, and several genes, such as galactinol synthases, which catalyze the first step in the pathway of raffinose synthesis, are not represented on the chip. In the case of Leu, the amino acid was not significantly altered during the anthesis stage but increased thereafter. This was somewhat in contrast with the behavior of transcripts associated with its synthesis, for example, the gene encoding 2-isopropylmalate synthase increases constantly during development, while several branched-chain amino acid transaminases were downregulated. This likely reflects a multilevel regulation of the branched-chain amino acids and suggests that the control resident in this metabolic network shifts among the constituent enzymes during the developmental period.

Integration of Metabolite and Transcript Profiling Data Obtained during Pollination-Independent Fruit Set

We next searched for consistent changes occurring when comparing the metabolites and transcripts of the transgenic line to that of the wild type. In this instance, not only the major sugars but also the minor sugars altered during development. An interesting example is the increased production of xylose in the antisense line during the later stages of development, which might be controlled by the upregulation of both dual-activity UDP-D-apiose/UDP-D-xylose synthase and UDP-D-xylose synthase isoforms in the transgenic line, since these enzymes represent both known synthetic pathways for xylose. As opposed to many other nucleotide sugar converting enzymes, it is anticipated that these enzymes catalyze irreversible reactions that would likely require tight regulatory control (Reiter, 2008). Another example in which the transgenic situation was somewhat different from that of the wild type is that the sharp rise in Leu synthesis, particular at the anthesis stage, could be explained in the antisense line by a concerted upregulation of 3-isopropylmalate dehydrogenase and 2-isopropylmalate synthase and a downregulation of Leu degrading enzymes, such as 3-methylcrotonyl-CoA carboxylase. These changes thus corroborate the hypothesis we made on the basis of the wild-type data alone, that Leu metabolism is controlled by multilevel regulation.

As observed for pollination-dependent fruit set, there were several changes in transcripts associated with ascorbate metabolism. While the metabolite L-galactono-lactone was increased in the antisense line at anthesis, the transcripts involved in the initial stages of the ascorbate synthesis pathway as well as the potential myo-inositol pathway were upregulated in the transgenic lines. However, in this instance, these transcriptional changes were not reflected in changing ascorbate levels. Moreover, it was observed that Arg decarboxylases were downregulated, while spermidine synthases were upregulated at this time point when comparing to the pollination dependent fruit set. Once again, this was not reflected in changes in the metabolites themselves. Figure 13C clearly highlights the differences between the two genotypes, revealing the dramatic upregulation of photosynthesis in the *IAA9* transgenics as well as an upregulation of glycerate 3-phosphate and the sugars sucrose, glucose, and fructose.

Differences between the Pollination-Dependent and -Independent Fruit Set Are More Discriminative at the Metabolomic Than the Transcriptomic Level

Having performed an integrative analysis, we next decided to compare the discriminatory power of the metabolite and transcript data sets independently. Principal component analysis of the 480 transcripts whose expression is significantly altered between pollination-dependent and -independent fruit set (Figure 14A) allowed clear discrimination of developmental stages along both the first and second principal component, leading to three separated groups corresponding to bud (light-gray circle), anthesis (red and dark-gray circles), and postanthesis stages (green circle). However, they could not discriminate between the wild type and *AS-IAA9* (AS) at bud and postanthesis stages, while at anthesis stage, wild-type (dark-gray circle) and *AS-IAA9* (red circle) were clearly separated along the two principal components. It indicates that at the global transcriptional level, there are no significant differences between fertilization-dependent and -independent fruit set but rather specific functional changes that are sufficient to mediate the observed phenotypic responses.

Principle component analysis (PCA) of metabolite data (Figure 14B) allowed clear discrimination both between the two genotypes and between the various stages of fruit set process. Wild-type samples (gray and black spots) could be discriminated from that of *AS-IAA9* (colored spots) along both the first and second principal component, highlighting the global differences in terms of metabolic changes between fertilization-dependent and fertilization-independent fruit set. Along the first principal component, the postanthesis stage separate from the earlier time points in both genotypes. In the wild type, they could not however discriminate anthesis from bud stages (gray circle); by contrast, *AS-IAA9* displayed a clear separation of anthesis (red circle) from bud stage (yellow circle), displaying a precocious shift of metabolite levels in *AS-IAA9*, consistent with the precocious development previously observed in these lines. Evaluation of the metabolites that made the major contribution to the discrimination observed in this graph revealed that they were components of cell wall and energy metabolism.

DISCUSSION

This study was designed to harness transcript and metabolite profiling technologies to evaluate changes occurring within the developing ovary and fruits of both wild-type and *AS-IAA9* plants to discriminate between fertilization-dependent and -independent fruit set. The underlying rationale was that such a study

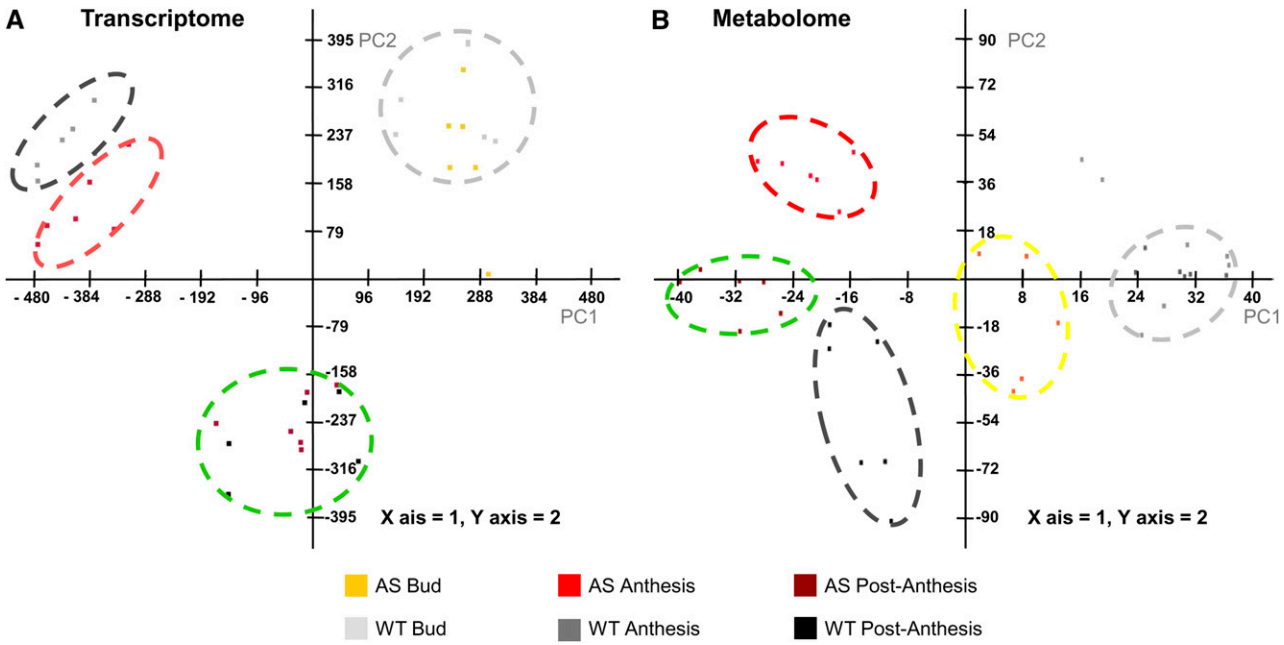

Figure 14. PCA of Transcripts and Metabolites during the Flower-to-Fruit Transition.

Score plot of two principle components of transcripts and metabolites showing that developmental stages as well as different genotypes (wild type and *AS-IAA9*) cluster separately.

(A) PCA of the 480 significantly altered transcript levels between AS1 and wild-type lines at all three developmental stages (see Venn diagram in Figure 5). Changes during development allow discrimination of developmental stages, leading to three separated groups corresponding to bud (light-gray circle), anthesis (red and dark-gray circle), and postanthesis stages (green circle).

(B) PCA of metabolite data. Wild-type samples clustered in two groups corresponding to bud/anthesis (gray) and postanthesis (black), while *AS-IAA9* samples clustered into three groups corresponding to bud (yellow), anthesis (red), and postanthesis (green).

could provide a valuable resource for understanding how IAA9 exerts its function on gene transcription and subsequently on primary metabolite accumulation and developmental processes. The data published so far on *Aux/IAA* genes have provided relatively little information concerning their in vivo function and the A*S-IAA9* transgenic lines and therefore represent a unique genetic resource in which the IAA9-mediated auxin response is effectively constitutive. It should be noted that this study has been performed with the MicroTom cultivar of tomato. This cultivar is developing into a useful research tool with many studies, documenting that it is essentially equivalent to larger nonmutated cultivars (Obiadalla-Ali et al., 2004a; Dan et al., 2005; Tsugane et al., 2005). The MicroTom background harbors several genetic mutations, including a floral meristem determinancy mutation and a brassinosteroid mutation (Meissner et al., 1997). However, given that our previous work showed that the altered fruit set phenotype in the antisense lines was fully reproducible in another genetic background (Wang et al., 2005), the use of MicroTom should not greatly complicate the interpretation of the results presented here.

The nature of the signals and sequence of events that stimulate or limit the processes involved in fruit initiation remain largely unknown, and the genes and mechanisms involved in translating the signal for fruit initiation evoked either by natural pollination or application of hormones, such as auxin and GAs, are still obscure. The vast majority of studies on fruit initiation focused on hormonal regulation and parthenocarpic fruit set (Vivian-Smith and Koltunow, 1999; Pandolfini et al., 2002; Wang et al., 2005; Goetz et al., 2006; Marti et al., 2007; Serrani et al., 2007, 2008; de Jong et al., 2009), though the effect of altering the flavonoid pathway has also been reported to lead to parthenocarpic fruit (Schijlen et al., 2006). However, to date, relatively few studies have used genomic tools to look at the global transcriptomic changes associated with flower-to-fruit transition (Vriezen et al., 2008). Other studies implementing a transcriptomic approach focused on the events occurring from 8 d after pollination onward and addressed more specifically either the expansion phase (Lemaire-Chamley et al., 2005) or later fruit development and ripening phases (Alba et al., 2005; Carrari et al., 2006).

Recent work in tomato revealed that downregulation of *IAA9* results in the uncoupling of fruit set from pollination and fertilization, thus giving rise to seedless (parthenocarpic) fruit. These data indicated that IAA9 is likely to participate within a regulatory complex that negatively regulates fruit initiation (Wang et al., 2005). IAA9 is a member of the Aux/IAA family constituting short-lived transcription factors involved in auxin response (Abel et al., 1995; Gray et al., 2001). The rapid turnover of these proteins allows exquisite control of the auxin response in plants (Dharmasiri and Estelle, 2002; Dreher et al., 2006), with their levels being mediated at both transcriptional and posttranslational levels. In this study, we used in situ mRNA hybridization to allow spatial resolution of the expression gradient of *IAA9* during fruit organogenesis. This expression was elevated in the ovary and peaked in specific tissues, such as the placenta, funiculus, and the inner layer of integument in the embryo sac. Within the mature flower, a distinctive expression gradient was apparent, and upon successful pollination and fertilization, this gradient was released with *IAA9* expression being spread across all tissues of the developing ovary/fruit. However, in the absence of fertilization, this gradient persisted, providing evidence that the initiation of normal fruit development and enlargement requires the dissipation of the *IAA9* mRNA gradient, thus suggesting an important regulatory role for IAA9 in the process of fruit set. Although we have yet to examine IAA9 protein levels, we speculate that prior to pollination and fertilization, *IAA9* transcripts (and proteins) are kept at a normal level but that following perception of the fertilization signal the IAA9 protein is rapidly and extensively degraded. While the rapid postfertilization decline in transcript levels is in keeping with this hypothesis, further experiments will be necessary to directly delineate the mechanism linking the fertilization signal to alterations in *IAA9* transcript abundance and ultimately to fruit set and growth. The observation that *IAA9* gradients persist in unfertilized ovules indicates that the negative regulation of fruit set by IAA9 is active throughout the flower-to-fruit transition, indicating a central role for the ovule in the mediation of fruit development.

The data documented both here and in our previous work (Wang et al., 2005) provide compelling arguments on the important role of auxin in the early events of tomato fruit development. It has been recently demonstrated that the interaction between Aux/IAA proteins and ARFs is instrumental in auxin-dependent transcriptional regulation (Tiwari et al., 2004; Dharmasiri et al., 2005). The identity of the exact ARF(s) putatively interacting with IAA9 is currently unknown, but a likely candidate is the protein encoded by the tomato ortholog of *Arabidopsis* ARF8. Indeed, recent studies have revealed that the parthenocarpic mutant *fwf*, which harbors a lesion in *ARF8*, exhibits an uncoupling of fruit set and growth from pollination and fertilization events (Goetz et al., 2006). Notably, ectopic expression in the tomato of an aberrant form of the *Arabidopsis ARF8* induces parthenocarpic fruit set (Goetz et al., 2007). Under normal circumstances, pollination is known to induce increases in the levels of both auxin and ethylene in floral organs, correlating with the observation of subsequent growth (O'Neill, 1997; Llop-Tous et al., 2000). It is thus conceivable that in wild-type flowers, an auxin burst induced by pollination and fertilization leads to the degradation of IAA9 protein via a proteolytic pathway such as that described for *Arabidopsis* (Woodward and Bartel, 2005). This scenario would thus be anticipated to abolish the repression of crucial auxin-responsive fruit initiation genes by the ARF-IAA9 protein complex. In the *AS-IAA9* lines, however, such a mechanism of repression is clearly impaired. It seems likely that the very low abundance of IAA9 in these lines is not capable of forming the inhibitory complex of ARF-IAA9 and thus leads to constitutive activation of auxin-responsive and fruit initiation genes. The ultimate consequence of this lack of control is fruit set in the absence of fertilization and subsequent parthenocarpy. In support of an active role of auxin during the flower-to-fruit transition, our data reveal that many transcriptional regulators from both ARF and Aux/IAA type undergo dramatic shifts in their expression throughout natural fruit set, suggesting that the coordinated regulation of these genes is integral to this developmental process.

Comprehensive transcriptomic profiling of the flower-to-fruit transition identified a large number of genes that are common to both pollination-induced and pollination-independent fruit set, among which only a small subset are IAA9 dependent. This

highlights the fact that a minimal change in gene expression can have a dramatic effect on the developmental fate of the flower organ. In contrast with pollination-induced fruit set, where the highest transition occurs between anthesis and postanthesis, the major shift in terms of changes in both transcript and metabolite accumulation in *AS-IAA9* occurs at the bud-to-anthesis transition. In accordance with this, functional categorization of the differentially expressed genes in both pollination-induced and pollination-independent fruit set reveals that the major groups of genes affected are related to signal transduction, metabolic pathways, and cell division. These results suggest that the fruit set process in tomato requires complex regulatory control and reconfiguration of metabolic processes. Evaluating the genes that are differentially expressed between wild-type and *AS-IAA9* lines during the flower-to-fruit transition revealed that the differences between the two lines are greatest at the anthesis stage. These data may explain why *AS-IAA9* enter the fruit differentiation process earlier than the wild type and with no requirement for pollination/fertilization signal.

Among the large number of transcription factors recruited during the process of fruit set in the wild type, the category of MADS box genes is the most striking regarding their sharp downregulation. Notably, *TAG1* and *TAGL6* genes undergo dramatic downregulation following fertilization, and the levels of their transcripts remain low throughout the early stages of fruit development. It has been reported that the *Agamous* gene takes part in the control of fruit organogenesis in *Arabidopsis* (Mizukami and Ma, 1992), and downexpression of *TM29*, another MADS box gene in the tomato, results in parthenocarpic fruit development (Ampomah-Dwamena et al., 2002). Moreover, downregulation of *TAG1* expression in tomato via antisense strategy results in dramatic alteration of flower development with conversion of stamens into petaloid organs and indeterminate growth of the floral meristem as well as in strong reduction of seed production (Pnueli et al., 1994). Given their dramatic downregulation during both pollination-dependent and -independent fruit set, *TAG1* and *TAGL6* genes emerge as potential active players in the process of fruit set. Moreover, since the transcript levels of both MADS box genes is low in *AS-IAA9* compared with the wild type, it is possible that this low expression promotes fruit set even in the absence of flower fertilization. Whether *IAA9* acts in concert with these MADS box genes to control fruit set initiation and whether auxin directly regulates their expression remains to be clarified.

In accordance with the precocious development of the ovary in *AS-IAA9*, a number of cell division–related genes show upregulation at anthesis stage in antisense lines, while their activation only occurs at postanthesis in wild-type lines. Following the same lines of evidence, the expression of two histone and two ribosomal protein genes was upregulated at both bud and anthesis stages in *AS-IAA9* but only at postanthesis in the wild type, again indicating that cell division may well have been boosted in the pollination-independent process.

The changes in transcript accumulation of a number of *ARF* and *Aux*/*IAA* genes are clearly indicative of active auxin signaling throughout the process of fruit set. Our data also reveal that auxin and ethylene-related genes are the most predominantly altered in terms of change in transcript accumulation with comparatively only few changes concerning GA. This brings ethylene into the field as a potential major player in coordinating the process of fruit set. It has long been reported that flower pollination induces a burst of ethylene production (Pech et al., 1987), though the role of this in fruit set has not been resolved. More recently, a transcriptomic profiling of fruit set identified ethylene-related genes among the most altered during fruit set (Vriezen et al., 2008). Downregulation of auxin-related genes occurs earlier (2 DPA) than that of ethylene-related genes (6 DPA), suggesting the existence of a temporal dependence on hormone action for the flower-to-fruit transition to proceed properly.

Another striking feature revealed by both metabolomic and transcriptomic profiling is related to aspects of photosynthesis and sugar metabolism during the flower-to-fruit transition. Given the widely documented crosstalk between hormone and sugar signaling (Arenas-Huertero et al., 2000; Leon and Sheen, 2003), it is highly interesting that the antisense lines were additionally characterized as being upregulated in the sucrose synthase pathway of sucrose degradation. This pathway is more energy efficient than that mediated by invertase (Bologa et al., 2003) and is likely the prominent pathway of sucrose degradation in later stages of development of many heterotrophic tissues, including tomato (Hackel et al., 2006). Thus, the observed elevation of the transcripts of this pathway could, at least partially, explain the precocious nature of fruit development in the transgenics. Two possible explanations could account for the observed elevation in the levels of sucrose, glucose, and fructose in the antisense lines: (1) it could be the consequence of a more efficient downloading of photoassimilate from the fruit, as observed on the introgression of a wild species allele of cell wall invertase (Fridman et al., 2004), or (2) it could be due to an increase in the fruits own photoassimilate production. The strong activation of photosynthesis-related genes during fruit set in *IAA9* downregulated lines is a major phenomenon. Strikingly, the activation of photosynthesis-related genes is delayed to the postanthesis stage in the wild type but takes place at the bud stage in *AS-IAA9*. Many recent studies have endorsed the prevailing opinion that fruit growth and metabolism are predominantly supported by photoassimilate supply from source tissues (Farrar et al., 2000; Nunes-Nesi et al., 2005; Schauer et al., 2006). However, it is important to note that the carpel of the fruit is essentially a modified leaf that has folded into a tubular structure enclosing the ovules (Bowman et al., 1991; Gillaspy et al., 1993) and that cells in developing fruit contain photosynthetically active chloroplasts and express both nuclear-encoded and plastidially encoded genes for photosynthetic proteins (Piechulla et al., 1987). Furthermore, combination of indirect evidence provides support for the hypothesis that during early developmental fruit, photosynthesis itself may provide a considerable contribution to both metabolism and growth of the organ (Tanaka et al., 1974; Obiadalla-Ali et al., 2004b). Recent studies have indicated that in tomato pericarp cells, the induction of genes related to photosynthesis and chloroplast biogenesis positively correlate with chloroplast numbers and cell size (Kolotilin et al., 2007). The results of this study provide compelling evidence that fruit photosynthesis plays an important role in fruit establishment. It is likely that the end phenotype of the lines is additionally influenced by the upregulation of the sucrose synthase pathway

of sucrose degradation since alterations of sucrose metabolism have often been correlated with changes in yield parameters (Lytovchenko et al., 2007). The combined data provide compelling evidence that photosynthesis is upregulated at the level of gene expression and that this is concurrent with a precocious fruit set and growth advantage in the antisense lines. It is dangerous to conclude causality on the basis of consistency analysis alone; therefore, we are generally not inclined to speculate as to whether the transcriptional change causes the metabolic one or vice versa. However, since it is extensively documented that high sugar contents repress photosynthesis (for review, see Rolland et al., 2006), in this instance, we can effectively exclude that the observed increases in sugars cause the observed increases in transcription of genes associated with photosynthesis. When taken alongside the altered growth rate, these data convincingly suggest that the transcriptional upregulation of photosynthesis is a key event required to sustain the fruit set developmental process. Consistent with this hypothesis is the fact that other features of the metabolite profiles of the transgenics reflect conditions that could be anticipated to promote photosynthesis and growth; for example, the observed changes in ascorbate and carbon nitrogen metabolism are diagnostic of conditions favoring efficient photosynthesis (for example, see Nunes-Nesi et al., 2005), while the elevation of intermediates of both ascorbate and shikimate pathways in the transformants are additionally consistent with the exhibited elevated growth. Ascorbate metabolism is one of the few pathways in which a clear association between changes at the levels of transcripts correlates with changes in metabolites. While the structural features of plant ascorbate biosynthesis are currently being clarified (for reviews, see Smirnoff et al., 2000; Ishikawa et al. 2006), the results from this study could well shed light on the regulation of this important pathway. At the transcriptional level, both galactose-dehydrogenase (L-Gal-DH) and GDP-L-galactose-hexose-1-phosphate guanyltransferase displayed clear differences that correlated well with the absolute ascorbate level, implying that these enzymes are likely highly important in determining the final level of this metabolite. The latter enzyme was recently cloned and suggested to be very important in determining the final ascorbate content (Laing et al., 2007). The other clear example of transcriptional regulation of metabolite content is provided by the polyamines, which seem to be particularly important in pollination-dependent fruit set. The inclusion of this class of metabolites as important regulators of fruit development is not without precedent since they have long been described to play an ethylene-dependent (Saftner and Baldi, 1990) role in flowering and fruit ripening (Kakkar and Rai, 1993). While more recent studies have revealed that engineering high fruit polyamine content enhances both the vine life and the nutritional content of tomato (Mehta et al., 2002), it has been recognized that pollination-independent fruit set in tomato is accompanied by a change in polyamine metabolism and that polyamine metabolism in general proves to be an interesting example for metabolite-enzyme activity correlation (Egea-Cortines et al., 1993). Despite the identification of these interesting correlations between transcript and metabolite level, it is clear that understanding the mechanisms of regulation of both these pathways and assessing their functional importance with respect to the fruit set developmental process will require substantial further work.

So far, only few molecular components of the flower-to-fruit transition have been described (Wang et al., 2005; Goetz et al.,

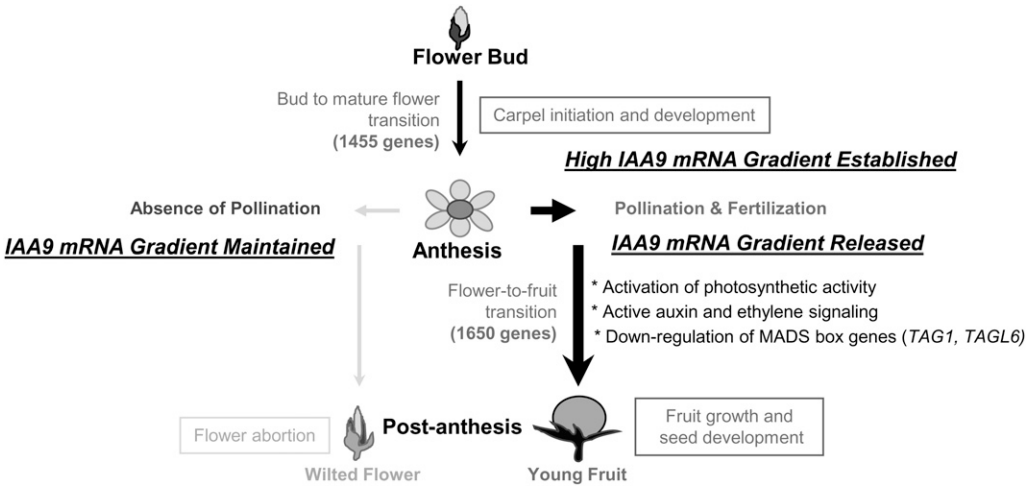

Figure 15. Model for Regulatory Events Underlying the Fruit Set Process in Tomato.

IAA9 regulates the initiation of fruit set by establishing a spatial expression gradient whose release triggers the flower-to-fruit transition. Transcriptomic and metabolomic analysis reveal novel regulatory points in pathways associated with natural pollination fruit set and pollination-independent fruit set. The comparative analysis at the transcriptomic and metabolic levels of pollination-induced and fertilization-free fruit set identifies auxin and ethylene signaling as well as photosynthesis and sugar metabolism as major events of the fruit set program and potential components of the regulatory mechanism underlying this developmental process. The downregulation of MADS box transcription factors (TAG1 and TAGL6) also emerges as a key event of the fruit set process.

2006; Pandolfini et al., 2007), and little is known concerning the overarching regulatory mechanisms that underpin this transition. Our study brings new insights not only on global biochemical and molecular events underlying this process, but also on their hormonal regulation. The model presented in Figure 15 highlights the role of *IAA9* expression and distribution in triggering ovary development into young fruit. Pollination induces a net release of the *IAA9* mRNA gradient that leads to the activation of the fruit set program, including changes in gene expression and metabolite accumulation. Of particular note were the concerted changes at transcript and metabolite levels of photosynthetic and sugar metabolism. The coupling of these changes to increased growth suggests that they may also be components of the control of the initiation of fruit development. In parallel, both auxin and ethylene signaling emerge as the main hormonal regulation events involved in the flower-to-fruit transition; however, the contribution albeit to a lesser extent of other phytohormones cannot be excluded. When taken together the combined data reported here suggest that IAA9 exerts a profound influence on the flower-to-fruit transition by, either directly or indirectly, affecting a substantial number of transcription factors belonging to ARF and Aux/IAA families and by downregulating the expression of *TAG1* and *TAGL6* MADS box genes. However, although IAA9 only affects a small number of transcriptional events, these changes provoke dramatic changes both at the levels of development and primary metabolism during the period of fruit set and subsequent early fruit growth. As such, these results allow a far greater comprehension of the molecular events controlling early fruit development both in the presence and absence of fertilization.

METHODS

Plant Material and Experimental Design

Tomato plants (*Solanum lycopersicum* cv MicroTom) and two independent homozygote lines of *AS-IAA9* were grown under standard greenhouse conditions (14-h-day/10-h-night cycle, 25/20°Cday/night temperature, 80% humidity, and 250 μmol m^{-2} s^{-1} light intensity). Flower emasculation was performed before dehiscence of anthers (closed flowers) to avoid accidental self-pollination. At all three stages (bud, anthesis, and postanthesis), only the ovary, including style and stigma, or developing young fruits were collected as samples. At the flower bud stage, the ovaries were collected just before anthesis (closed flowers). Anthesis stage samples were collected on the first day of flower opening. Stage-specific pooled samples (>50 ovary/fruit) were divided into two groups, with one group being used for transcriptome profiling experiments and the other one for metabolite profiling experiments.

Histological Analysis

For histological analysis, flower buds of 0.5 to 8 mm in length were fixed in FAA solution (4% paraformaldehyde, 50% ethanol, and 5% acetic acid in 1× PBS), placed under vacuum for 10 min, and incubated overnight at 4°C before being dehydrated in alcohol and embedded in paraffin (Paraplast plus; Sigma-Aldrich). At least 10 buds were sampled and checked for each stage of development. Histological preparations were performed according to Baldet et al. (2006). For histological analysis, 80-μm-thick sections were stained with 0.05% toluidine blue. Slides were observed under a microscope (Zeiss-Axioplan).

In Situ Hybridization

A 246-bp fragment from the 3′ untranslated region of *IAA9* was amplified with primers *IAA9*_inF (5′- AGGGCTATGGAAAAGTGTCGGAGCAGA-AAT-3′) and *IAA9*_inR (5′-AACTTAAAAGAGGACATATATTACGCA -3′) and cloned into pGEM-T easy. Plasmids were sequenced to verify identity and orientation of inserts. Sense (control) and antisense digoxygenin-labeled probes were generated by run-off transcription using SP6 RNA polymerases according to the manufacturer's protocol (Roche Diagnostics). For in situ hybridization, tomato flower buds were sampled and processed as described by Baldet et al. (2006).

RNA Extraction

Total RNA was isolated from ovary/young fruits using an RNA exaction kit (RNeasy plant mini kit; Qiagen) and was DNase-treated according to the manufacturer's protocol (RNase-Free DNase Set; Qiagen).

Microarray Experiment Analysis

For each developmental stage collected, we did direct comparison of *AS-IAA9* line AS1 with their normal counterpart using two-color hybridizations onto EU-TOM1 microarray slides. The EU-TOM1 chip contains 11,860 different 70-mers oligonucleotides. The majority of the probes were designed from gene sequences gathered from the Lycopersicon Combined Build #3 Unigene database at Cornell University (http://www.sgn.cornell.edu/unigene_builds/).

Labeled cDNA was prepared according to the Pronto Plus direct system protocol (Promega). Five micrograms of total RNA was used for each labeling reaction. Labeled probes were annealed to the target oligonucleotides for 14 to 16 h at 42°C. Arrays were washed twice at 42°C (90 s and 5 min, respectively) in 2× SSC/0.1% SDS and then twice for 2 min in 1× SSC and twice for 1 min in 0.1× SSC at ambient temperature. Slides were then dried by centrifugation (5 min to 800 rpm). For each of the three stages, three biological repeats were performed in dye-swap experiments (total of 18 hybridizations). Dye bias was minimized by conducting half of the replicate hybridizations with wild-type cDNAs labeled with Cy3 and half with Cy5. Images were acquired using a Genepix 4000A microarray scanner (Molecular Devices) at 10-μm resolution per pixel, adjusting the photomultiplier tension to achieve optimal distribution of the signal and few number of saturated spots. Quantification was performed with Genepix Pro 3 software (Molecular Devices).

To identify genes that are differentially expressed between wild-type and *AS-IAA9* lines, analysis was done in R (http://www.r-project.org/) using modules from the BioConductor R/MAANOVA package (Kerr et al., 2000). Microarray intensities were $\log_2$ tranformed and normalized using LOWESS algorithm to remove intraslide dye bias. This preprocessed data set was then analyzed using the R/MAANOVA package with a fixed model and array, dye, and sample (ASvsWT) as covariables. For selection of differentially expressed genes, false discovery rate corrected permutation P values (500 permutations) were employed (Benjamini and Hochberg, 2001). Among these genes, only those displaying a $\log_2$ (ratio) higher than 0.5 or lower than −0.5 were retained, which corresponds to fold difference >1.4. R/MAANOVA analysis was selected as the statistical method of choice since it permits the separate consideration of array and dye effects as experimental covariables, omitting the requirement for inter-slide normalization approaches, notoriously known to introduce artificial bias (Woo et al., 2005). In the case, where the development of only the wild-type or only the antisense lines were considered, the background was subtracted from the foreground signal; afterwards, the red and green channels were decoupled and either all channels describing antisense line or all channels describing wild-type expression were $\log_2$ transformed and these values were quantile normalized. To these quantile normalized values a linear model was fitted using the limma package

taking technical replicates into account, and P values were determined using the empirical Bayes procedure as implemented in the limma package (Smyth, 2004).

Real-Time qRT-PCR Reactions

The same total RNA samples extracted for the microarray experiment were used to synthesize cDNA templates required for qRT-PCR analysis. cDNA synthesis was performed using a qRT-PCR cDNA synthesis kit (Ominiscript Reverse Transcription; Qiagen). Gene-specific primers were designed using Primer Express software Applied Biosystems (see Supplemental Table 8 online). qRT-PCRs were performed using SYBR GREEN PCR master mix (Applied Biosystems) on an ABI PRISM 7900HT sequence detection system. For all real-time PCR experiments, at least three biological replicates were performed, and each reaction was run in triplicate. Relative fold differences were calculated based on the comparative Ct (threshold constant) method using Sl-Actin-51 (accession number Q96483) as an internal standard with primers Actin _F (5′-TGTCCCTATTTACGAGGGTTATGC-3′) and Actin_R (5′-AGTTAAATCACGACCAGCAAGAT-3′). To determine relative fold differences for each sample in each experiment, the Ct value for each gene was normalized to the Ct value for Sl-Actin-51 and was calculated relative to a calibrator using the equation $2^{-\Delta\Delta Ct}$.

Metabolite Analysis

Metabolite extraction was performed as described previously (Roessner et al., 2001; Schauer et al., 2006). One hundred milligrams of tomato tissue from the three developmental stages were homogenized using a ball mill precooled with liquid nitrogen. Derivatization and GC-MS analysis were performed as described previously (Lisec et al., 2006). The GC-MS system was comprised of a CTC CombiPAL autosampler, an Agilent 6890N gas chromatograph, and a LECO Pegasus III TOF-MS running in EI+ mode. Metabolites were identified in comparison to database entries of authentic standards (Schauer et al., 2005b). Recovery experiments concerning the validity of the extraction and processing have been documented previously (Schauer et al., 2005a). If two observations from the metabolite data set are described in the text as different, this means that their difference was determined to be statistically significant ($P < 0.05$) by the performance of Student's *t* test using the algorithm incorporated into Microsoft Excel 7.0. PCA was performed using the informatic program MeV 4.0 (Saeed et al., 2003)

Metabolite-Transcript Consistency Analyses

To find links between metabolites and transcripts, a consistency analysis was performed on the basis of biological pathway knowledge essentially as detailed by Gibon et al. (2006). For this purpose, metabolites that were differentially abundant under the experimental conditions evaluated were identified, and transcripts coding for enzymes involved in the metabolism of the compound in question were extracted from the entire data sets using MapMan (Usadel et al., 2005). Subsequently, the tomato mapping files for MapMan (Urbanczyk-Wochniak et al., 2005) were used to visualize relevant pathways and to judge consistency between changes in metabolite and transcript levels by displaying both levels of information at the same time. In brief, the data sets were loaded into PageMan. First, the whole data set, including metabolites and transcripts, was analyzed for a consistent up- or downregulation. This was done Bin and subbin-wise using a Wilcoxon test with Benjamini Hochberg type false discovery rate control using the built-in PageMan function. The metabolite data were then added separately by averaging bin-wise, thus enabling the display of metabolites individually but also the visualization of their contribution to individual bins.

Accession Number

Microarray data have been deposited in the Array-Express public repository with the access number E-MEXP-1617.

Supplemental Data

The following materials are available in the online version of this article.

Supplemental Figure 1. Visualization of Ala Synthesis.

Supplemental Figure 2. Visualization of His Synthesis.

Supplemental Figure 3. Visualization of Asp Metabolism.

Supplemental Table 1. Differentially Expressed Genes during Natural Pollination-Dependent Fruit Set in the Wild Type.

Supplemental Table 2. Differentially Expressed Genes during Pollination-Independent Fruit Set in *AS-IAA9* Lines.

Supplemental Table 3. Differentially Expressed Genes between *AS-IAA9* Lines and the Wild Type in Ovary/Young Fruit.

Supplemental Table 4. Differentially Expressed Genes during Both Pollination-Dependent and -Independent Fruit Set.

Supplemental Table 5. IAA9 Regulated and Differentially Expressed Genes during both Pollination-Dependent and -Independent Fruit Set.

Supplemental Table 6. Relative Metabolites Contents during Pollination-Dependent and -Independent Fruit Set.

Supplemental Table 7. Validation of Microarray Expression Data by Quantitative RT-PCR.

Supplemental Table 8. Primers Used for qRT-PCR and the Accession Numbers of the Relevant Genes.

ACKNOWLEDGMENTS

This research was supported by the European Commission (EU-SOL Project PI 016214) and by the Midi-Pyrénées Regional Council (Grants 06003789 and 07003760). A.R.F. and M.B. were partially supported by the France-Germany-Spain Trilateral, and A.R.F. and N.S. were supported by a Deutsche-Israeli Project grant. We thank L. Tessarotto, H. Mondiès, O. Berseille, and D. Saint-Martin (Institut National Polytechnique Toulouse) for tomato genetic transformation and plant growth, L. Trouilhet (Toulouse Midi Pyrénées Genopole) for the production of tomato oligomicroarray slides, and S. Sokol (Toulouse Midi Pyrénées Genopole) for helping in microarray data analysis.

Received May 16, 2008; revised March 16, 2009; accepted April 24, 2009; published May 12, 2009.

REFERENCES

Abel, S., Nguyen, M.D., and Theologis, A. (1995). The PS-IAA4/5-like family of early auxin-inducible mRNAs in *Arabidopsis thaliana*. J. Mol. Biol. **251:** 533–549.

Alba, R., Payton, P., Fei, Z., McQuinn, R., Debbie, P., Martin, G.B., Tanksley, S.D., and Giovannoni, J.J. (2005). Transcriptome and selected metabolite analyses reveal multiple points of ethylene control during tomato fruit development. Plant Cell **17:** 2954–2965.

Ampomah-Dwamena, C., Morris, B.A., Sutherland, P., Veit, B., and Yao, J.L. (2002). Down-regulation of TM29, a tomato SEPALLATA

homolog, causes parthenocarpic fruit development and floral reversion. Plant Physiol. **130:** 605–617.

Arenas-Huertero, F., Arroyo, A., Zhou, L., Sheen, J., and Leon, P. (2000). Analysis of Arabidopsis glucose insensitive mutants, gin5 and gin6, reveals a central role of the plant hormone ABA in the regulation of plant vegetative development by sugar. Genes Dev. **14:** 2085–2096.

Baldet, P., Hernould, M., Laporte, F., Mounet, F., Just, D., Mouras, A., Chevalier, C., and Rothan, C. (2006). The expression of cell proliferation-related genes in early developing flowers is affected by a fruit load reduction in tomato plants. J. Exp. Bot. **57:** 961–970.

Benjamini, Y., and Hochberg, Y. (2001). The control of the false discovery rate in multiple testing under dependency. Ann. Stat. **29:** 1165–1188.

Bologa, K.L., Fernie, A.R., Leisse, A., Loureiro, M.E., and Geigenberger, P. (2003). A bypass of sucrose synthase leads to low internal oxygen and impaired metabolic performance in growing potato tubers. Plant Physiol. **132:** 2058–2072.

Bowman, J.L., Smyth, D.R., and Meyerowits, M. (1991). Genetic interactions among floral homeotic genes of *Arabidopsis*. Development **112:** 1–20.

Carmi, N., Salts, Y., Dedicova, B., Shabtai, S., and Barg, R. (2003). Induction of parthenocarpy in tomato via specific expression of the rolB gene in the ovary. Planta **217:** 726–735.

Carrari, F., Baxter, C., Usadel, B., Urbanczyk-Wochniak, E., Zanor, M.I., Nunes-Nesi, A., Nikiforova, V., Centero, D., Ratzka, A., Pauly, M., Sweetlove, L.J., and Fernie, A.R. (2006). Integrated analysis of metabolite and transcript levels reveals the metabolic shifts that underlie tomato fruit development and highlight regulatory aspects of metabolic network behavior. Plant Physiol. **142:** 1380–1396.

Coombe, B.G. (1960). Relationship of growth and development to changes in sugars, auxins, and gibberellins in fruit of seeded and seedless varieties of *Vitis vinifera*. Plant Physiol. **35:** 241–250.

Dan, Y.H., Yan, H., Munyikwa, T., Dong, J., Zhang, Y.L., and Armstrong, C.L. (2005). MicroTom a high throughput model transformation system for functional genomics. Plant Cell Rep. **25:** 432–441.

de Jong, M., Wolters-Arts, M., Feron, R., Mariani, C., and Vriezen, W.H. (2009). The *Solanum lycopersicum* auxin response factor 7 (SlARF7) regulates auxin signaling during tomato fruit set and development. Plant J. **57:** 160–170.

Dharmasiri, N., Dharmasiri, S., and Estelle, M. (2005). The F-box protein TIR1 is an auxin receptor. Nature **435:** 441–445.

Dharmasiri, S., and Estelle, M. (2002). The role of regulated protein degradation in auxin response. Plant Mol. Biol. **49:** 401–409.

Dreher, K.A., Brown, J., Saw, R.E., and Callis, J. (2006). The *Arabidopsis* Aux/IAA protein family has diversified in degradation and auxin responsiveness. Plant Cell **18:** 699–714.

Dudareva, N., Cseke, L., Blanc, V.M., and Pichersky, E. (1996). Evolution of floral scent in Clarkia: Novel patterns of S-linalool synthase gene expression in the *C. breweri* flower. Plant Cell **8:** 1137–1148.

Dunphy, P.J. (2006). Location and biosynthesis of monoterpenyl fatty acyl esters in rose petals. Phytochemistry **67:** 1110–1119.

Egea-Cortines, M., Cohen, E., Arad, S., Bagni, N., and Mizrahi, Y. (1993). Polyamine levels in pollinated and auxin-induced fruit of the tomato (*Lycopersicon esculentum*) during development. Physiol. Plant. **87:** 14–20.

Farrar, J.F., Pollock, C., and Gallagher, J. (2000). Sucrose and the integration of metabolism in vascular plants. Plant Sci. **154:** 1–11.

Fridman, E., Carrari, F., Lui, Y.S., Fernie, A.R., and Zamir, D. (2004). Zooming in on a quantitative trait for tomato yield using interspecific introgressions. Science **305:** 1786–1789.

George, W.L., Scott, J.W., and Splittstoesser, W.E. (1984). Parthenocarpy in tomato. Hortic. Rev. (Am. Soc. Hortic. Sci.) **6:** 65–84.

Gibon, Y., Usadel, B., Blaesing, O.E., Kamlage, B., Hoehne, M., Trethewey, R.N., and Stitt, M. (2006). Integration of metabolite with transcript and enzyme activity profiling during diurnal cycles in Arabidopsis rosettes. Genome Biol. **7:** R76.

Gillaspy, G., Ben-David, H., and Gruissem, W. (1993). Fruits: A developmental perspectives. Plant Cell **5:** 1439–1451.

Giovannoni, J. (2001). Molecular biology of fruit maturation and ripening. Annu. Rev. Plant Physiol. Plant Mol. Biol. **52:** 725–749.

Goetz, M., Hooper, L.C., Johnson, S.D., Rodrigues, J.C., Vivian-Smith, A., and Koltunow, A.M. (2007). Expression of aberrant forms of AUXIN RESPONSE FACTOR8 stimulates parthenocarpy in Arabidopsis and tomato. Plant Physiol. **145:** 351–366.

Goetz, M., Vivian-Smith, A., Johnson, S.D., and Koltunow, A.M. (2006). AUXIN RESPONSE FACTOR8 is a negative regulator of fruit initiation in *Arabidopsis*. Plant Cell **18:** 1873–1886.

Gorguet, B., van Heusden, A.W., and Lindhout, P. (2005). Parthenocarpic fruit development in tomato. Plant Biol (Stuttg.) **7:** 131–139.

Gray, W.M., Kepinski, S., Rouse, D., Leyser, O., and Estelle, M. (2001). Auxin regulates SCF(TIR1)-dependent degradation of AUX/IAA proteins. Nature **414:** 271–276.

Gustafson, F.G. (1936). Inducement of fruit development by growth promoting chemicals. Proc. Natl. Acad. Sci. USA **22:** 628–636.

Hackel, A., Schauer, N., Carrari, F., Fernie, A.R., Grimm, B., and Kuhn, C. (2006). Sucrose transporter LeSUT1 and LeSUT2 inhibition affects tomato fruit development in different ways. Plant J. **45:** 180–192.

Ishikawa, T., Dowdle, J., and Smirnoff, N. (2006). Progress in manipulating ascorbic acid and accumulation in plants. Physiol. Plant. **126:** 343–355.

Kakkar, R.K., and Rai, V.K. (1993). Plant polyamines in flowering and fruit ripening. Phytochemistry **33:** 1281–1288.

Kerr, M.K., Martin, M., and Churchill, G.A. (2000). Analysis of variance for gene expression microarray data. J. Comput. Biol. **7:** 819–837.

Kolotilin, I., Koltai, H., Tadmor, Y., Bar-Or, C., Reuveni, M., Meir, A., Nahon, S., Shlomo, H., Chen, L., and Levin, I. (2007). Transcriptional profiling of high pigment-2dg tomato mutant links early fruit plastid biogenesis with its overproduction of phytonutrients. Plant Physiol. **145:** 389–401.

Laing, W.A., Wright, M.A., Cooney, J., and Bulley, S.M. (2007). The missing step of the L-galactose pathway of ascorbate biosynthesis in plants, an L-galactose guanyltransferase, increases leaf ascorbate content. Proc. Natl. Acad. Sci. USA **104:** 9534–9539.

Lemaire-Chamley, M., Petit, J., Garcia, V., Just, D., Baldet, P., Germain, V., Fagard, M., Mouassite, M., Cheniclet, C., and Rothan, C. (2005). Changes in transcriptional profiles are associated with early fruit tissue specialization in tomato. Plant Physiol. **139:** 750–769.

Leon, P., and Sheen, J. (2003). Sugar and hormone connections. Trends Plant Sci. **8:** 110–116.

Lisec, J., Schauer, N., Kopka, J., Willmitzer, L., and Fernie, A.R. (2006). Gas chromatography mass spectrometry-based metabolite profiling in plants. Nat. Protocols **1:** 387–396.

Llop-Tous, I., Barry, C.S., and Grierson, D. (2000). Regulation of ethylene biosynthesis in response to pollination in tomato flowers. Plant Physiol. **123:** 971–978.

Lytovchenko, A., Sonnewald, U., and Fernie, A.R. (2007). The complex network of non-cellulosic carbohydrate metabolism. Curr. Opin. Plant Biol. **10:** 227–235.

Marti, C., Orzaez, D., Ellul, P., Moreno, V., Carbonell, J., and Granell, A. (2007). Silencing of DELLA induces facultative parthenocarpy in tomato fruits. Plant J. **52:** 865–876.

Mehta, R.A., Cassol, T., Li, N., Ali, N., Hanada, A.K., and Mattoo, A.K. (2002). Engineered polamine accumulation in tomato enhances phytonutrient content, juice quality, and vine life. Nat. Biotechnol. **20:** 613–618.

Meissner, R., Jacobson, Y., Melame, S., Levyatuv, S., Shalev, G., Ashri, A., Elkind, Y., and Levy, A. (1997). A new model system for tomato genetics. Plant J. **12:** 1465–1472.

Mizukami, Y., and Ma, H. (1992). Ectopic expression of the floral homeotic gene AGAMOUS in transgenic Arabidopsis plants alters floral organ identity. Cell **71:** 119–131.

Moyano, E., Martinez-Garcia, J.F., and Martin, C. (1996). Apparent redundancy in myb gene function provides gearing for the control of flavonoid biosynthesis in antirrhinum flowers. Plant Cell **8:** 1519–1532.

Nitsch, J.P. (1970). Hormonal factors in growth and development. In The Biochemistry of Fruits and Their Products, A.C. Hulme, ed (New York: Academic Press), pp. 427–472.

Nunes-Nesi, A., Carrari, F., Lytovchenko, A., Smith, A.M.O., Loureiro, M.E., Ratcliffe, R.G., Sweetlove, L.J., and Fernie, A.R. (2005). Enhanced photosynthetic perfomance and growth as a consequence of decreasing mitochondrial malate dehydrogenase activity in transgenic tomato plants. Plant Physiol. **137:** 611–622.

Obiadalla-Ali, H., Fernie, A.R., Kossmann, J., and Lloyd, J.R. (2004a). Developmental analysis of carbohydrate metabolism in tomato (*Lycopersicon esculentum* cv. Micro-Tom) fruits. Physiol. Plant. **120:** 196–204.

Obiadalla-Ali, H., Fernie, A.R., Lytovchenko, A., Kossmann, J., and Lloyd, J.R. (2004b). Inhibition of chloroplastic fructose 1,6-bisphosphate in tomato fruits leads to decreased fruit size, but only small changes in carbohydrate metabolism. Planta **219:** 533–540.

O'Neill, S.D. (1997). Pollination regulation of flower development. Annu. Rev. Plant Physiol. Plant Mol. Biol. **48:** 547–574.

Ozga, J.A., van Huizen, R., and Reinecke, D.M. (2002). Hormone and seed-specific regulation of pea fruit growth. Plant Physiol. **128:** 1379–1389.

Pandolfini, T., Molesini, B., and Spena, A. (2007). Molecular dissection of the role of auxin in fruit initiation. Trends Plant Sci. **12:** 327–329.

Pandolfini, T., Rotino, G.L., Camerini, S., Defez, R., and Spena, A. (2002). Optimisation of transgene action at the post-transcriptional level: high quality parthenocarpic fruits in industrial tomatoes. BMC Biotechnol. **2:** 1.

Pech, J.C., Latche, A., Larrigaudière, C., and Reid, M.S. (1987). Control of early ethylene synthesis in pollinated petunia flowers. Plant Physiol. Biochem. **25:** 431–437.

Picken, A.J.F. (1984). A review of pollination and fruit set in the tomato (*Lycopersicon esculentum* Mill). J. Hortic. Sci. **59:** 1–13.

Piechulla, B., Glick, R.E., Bahl, H., Melis, A., and Gruissem, W. (1987). Changes in photosynthetic capacity and photosynthetic protein pattern during tomato fruit ripening. Plant Physiol. **84:** 911–917.

Pnueli, L., Hareven, A.D., Rounsley, S.D., Yanofsky, M.F., and Lifschitz, E. (1994). Isolation of the tomato agamous gene TAG1 and analysis of its homeotic role in transgenic plants. Plant Cell **6:** 163–173.

Potts, W.C., Reid, J.B., and Murfet, I.C. (1985). Internode length in Pisum: Gibberellins and the slender phenotype. Physiol. Plant. **63:** 357–364.

Reiter, W.D. (2008). Biochemical genetics of nucleotide sugar interconversion reactions. Curr. Opin. Plant Biol. **11:** 236–243.

Roessner, U., Luedemann, A., Brust, D., Fiehn, O., Linke, T., Willmitzer, L., and Fernie, A. (2001). Metabolic profiling allows comprehensive phenotyping of genetically or environmentally modified plant systems. Plant Cell **13:** 11–29.

Rolland, F., Baena-Gonzalez, E., and Sheen, J. (2006). Sugar sensing and signalling in plants: Conserved and novel mechanisms. Annu. Rev. Plant Biol. **57:** 675–709.

Rotino, G.L., Acciarri, N., Sabatini, E., Mennella, G., Lo Scalzo, R., Maestrelli, A., Molesini, B., Pandolfini, T., Scalzo, J., Mezzetti, B., and Spena, A. (2005). Open field trial of genetically modified parthenocarpic tomato: Seedlessness and fruit quality. BMC Biotechnol. **5:** 32.

Saeed, A., et al. (2003). TM4: A free, open-source system for microarray data management and analysis. Biotechniques **34:** 374–378.

Saftner, B.A., and Baldi, B.G. (1990). Polyamine levels and tomato fruit development - possible interaction with ethylene. Plant Physiol. **92:** 547–550.

Schauer, N., et al. (2006). Comprehensive metabolic profiling and phenotyping of interspecific introgression lines for tomato improvement. Nat. Biotechnol. **24:** 447–454.

Schauer, N., Steinhauser, D., Strelkov, S., Schomburg, D., Allison, G., Moritz, T., Lundgren, K., Roessner-Tunali, U., Forbes, M.G., Willmitzer, L., Fernie, A.R., and Kopka, J. (2005b). GC-MS libraries for the rapid identification of metabolites in complex biological samples. FEBS Lett. **579:** 1332–1337.

Schauer, N., Zamir, D., and Fernie, A.R. (2005a). Metabolic profiling of leaves and fruit of wild species tomato: a survey of the *Solanum lycopersicum* complex. J. Exp. Bot. **56:** 297–307.

Schijlen, E., Ric de Vos, C.H., Jonker, H., van den Broeck, H., Molthoff, J., van Tunen, A., Martens, S., and Bovy, A. (2006). Pathway engineering for healthy phytochemicals leading to the production of novel flavonoids in tomato fruit. Plant Biotechnol. J. **4:** 433–444.

Sedgley, M., and Griffin, A.R. (1989). Sexual Reproduction of Tree Crops. (London: Academic Press).

Serrani, J.C., Ruiz-Rivero, O., Fos, M., and Garcia-Martinez, J.L. (2008). Auxin-induced fruit-set in tomato is mediated in part by gibberellins. Plant J. **56:** 922–934.

Serrani, J.C., Sanjuan, R., Ruiz-Rivero, O., Fos, M., and Garcia-Martinez, J.L. (2007). Gibberellin regulation of fruit set and growth in tomato. Plant Physiol. **145:** 246–257.

Smirnoff, N., Conklin, P.L., and Loewus, F.A. (2000). Biosynthesis of ascorbate acid in plants: A renaissance. Annu. Rev. Plant Physiol. Plant Mol. Biol. **52:** 437–459.

Smyth, G.K. (2004). Linear models and empirical Bayes methods for assessing differential expression in microarray experiments. Stat. Appl. Genet. Mol. Biol. **3** (online) doi/10.2202/1544-6115.1027.

Talon, M., Zacarias, L., and Primo-Millo, E. (1992). Gibberellins and parthenocarpic ability in developing ovaries of seedless mandarins. Plant Physiol. **99:** 1575–1581.

Tanaka, A., Fujita, K., and Kikuchi, K. (1974). Nutriophysiological studies on the tomato plant, III. Photosynthetic rate of individual leaves in relation to the dry matter production of plants. Soil Sci. Plant Nutr. **20:** 173–183.

Tiwari, S.B., Hagen, G., and Guilfoyle, T.J. (2004). Aux/IAA proteins contain a potent transcriptional repression domain. Plant Cell **16:** 533–543.

Tsugane, T., Watanabe, M., Yano, K., Sakurai, N., Suzuki, H., and Shibata, D. (2005). Expressed sequence tags of full-length cDNA clonesfrom the miniature tomato (*Lycopersicon esculentum*) cultivar Micro-Tom. Plant Biotechnol. **22:** 161–165.

Urbanczyk-Wochniak, E., et al. (2005). Conversion of MapMan to allow the analysis of transcript data from Solanaceous species: Effects of genetic and environmental alterations in energy metabolism in the leaf. Plant Mol. Biol. **60:** 773–792.

Usadel, B., et al. (2005). Extension of the visualization tool MapMan to allow statistical analysis of arrays, display of corresponding genes, and comparison with known responses. Plant Physiol. **138:** 1195–1204.

Vivian-Smith, A., and Koltunow, A.M. (1999). Genetic analysis of growth-regulator-induced parthenocarpy in Arabidopsis. Plant Physiol. **121:** 437–451.

Vivian-Smith, A., Luo, M., Chaudhury, A., and Koltunow, A. (2001). Fruit development is actively restricted in the absence of fertilization in Arabidopsis. Development **128:** 2321–2331.

Vriezen, W.H., Feron, R., Maretto, F., Keijman, J., and Mariani, C. (2008). Changes in tomato ovary transcriptome demonstrate complex hormonal regulation of fruit set. New Phytol. **177:** 60–76.

Wang, H., Jones, B., Li, Z., Frasse, P., Delalande, C., Regad, F., Chaabouni, S., Latche, A., Pech, J.C., and Bouzayen, M. (2005). The tomato Aux/IAA transcription factor IAA9 is involved in fruit development and leaf morphogenesis. Plant Cell **17:** 2676–2692.

Woo, Y., Krueger, W., Kaur, A., and Churchill, G. (2005). Experimental design for three-color and four-color gene expression microarrays. Bioinformatics **21:** 459–467.

Woodward, A.W., and Bartel, B. (2005). Auxin: Regulation, action, and interaction. Ann. Bot. (Lond.) **95:** 707–735.